Integration of Bridge Damage Detection Concepts and Components

Volume II: Acceleration-Based Damage Detection

BRIDGE ENGINEERING CENTER

Final Report 2 of 3
October 2013

IOWA STATE UNIVERSITY
Institute for Transportation

THE UNIVERSITY OF IOWA

Sponsored by
Iowa Highway Research Board
(IHRB Project TR-636)
Iowa Department of Transportation
(InTrans Project 11-416)

About the BEC

The mission of the Bridge Engineering Center is to conduct research on bridge technologies to help bridge designers/owners design, build, and maintain long-lasting bridges.

Disclaimer Notice

Non-Discrimination Statement

Iowa Department of Transportation Statements

The preparation of this report was financed in part through funds provided by the Iowa Department of Transportation through its "Second Revised Agreement for the Management of Research Conducted by Iowa State University for the Iowa Department of Transportation" and its amendments.

Technical Report Documentation Page

1. Report No. IHRB Project TR-636	**2. Government Accession No.**	**3. Recipient's Catalog No.**
4. Title and Subtitle Integration of Bridge Damage Detection Concepts and Components Volume II: Acceleration-Based Damage Detection		**5. Report Date** October 2013 **6. Performing Organization Code**
7. Author(s) Salam Rahmatalla, Charles Schallhorn, and Ghedhban Swadi		**8. Performing Organization Report No.** InTrans Project 11-416
9. Performing Organization Name and Address Center for Computer-Aided Design College of Engineering University of Iowa Iowa City, IA 52242		**10. Work Unit No. (TRAIS)** **11. Contract or Grant No.**
12. Sponsoring Organization Name and Address Iowa Highway Research Board Iowa Department of Transportation 800 Lincoln Way Ames, IA 50010		**13. Type of Report and Period Covered** Final Report 2 of 3 **14. Sponsoring Agency Code** IHRB Project TR-636

15. Supplementary Notes

Visit www.intrans.iastate.edu for color pdfs of this and other research reports.

16. Abstract

In this work, a previously developed structural health monitoring (SHM) system was advanced toward a ready-for-implementation system. Improvements were made with respect to automated data reduction/analysis, data acquisition hardware, sensor types, and communication network architecture.

The objective of this part of the project was to validate/integrate a vibration-based damage-detection algorithm with the strain-based methodology formulated by the Iowa State University Bridge Engineering Center. This report volume (Volume II) presents the use of vibration-based damage-detection approaches as local methods to quantify damage at critical areas in structures.

Acceleration data were collected and analyzed to evaluate the relationships between sensors and with changes in environmental conditions. A sacrificial specimen was investigated to verify the damage-detection capabilities and this volume presents a transmissibility concept and damage-detection algorithm that show potential to sense local changes in the dynamic stiffness between points across a joint of a real structure.

The validation and integration of the vibration-based and strain-based damage-detection methodologies will add significant value to Iowa's current and future bridge maintenance, planning, and management

17. Key Words damage detection algorithm—failure-critical joints—local damage quantification—sacrificial specimen—SHM—structural health monitoring—temperature change effects—transmissibility ratios—vibration-based detection		**18. Distribution Statement** No restrictions.	
19. Security Classification (of this report) Unclassified.	**20. Security Classification (of this page)** Unclassified.	**21. No. of Pages** 44	**22. Price** NA

Form DOT F 1700.7 (8-72) **Reproduction of completed page authorized**

THREE-VOLUME REPORT ABSTRACT

The Iowa Department of Transportation (DOT) started investing in research (through both the Iowa Highway Research Board and the Office of Bridges and Structures) in 2003 to develop a structural health monitoring (SHM) system capable of identifying damage and able to report on the general operational condition of bridges. In some cases, the precipitous for these developments has been a desire to avoid damage that might go unnoticed until the next biennial inspection. Of specific and immediate concern was the state's inventory of fracture-critical structures.

The goal of this project was to bring together various components of recently-completed research at Iowa's Regent Universities with the following specific objectives:

- Final development of the overall SHM system hardware and software
- Integration of vibration-based measurements into current damage-detection algorithm
- Evaluation and development of energy-harvesting techniques

The following three volumes of the final report cover the results of this project:

Volume I: Strain-Based Damage Detection, from the Iowa State University Bridge Engineering Center, reviews information important to the strain-based SHM methodologies, details the upgraded damage-detection hardware and software system, demonstrates the application of the control-chart-based methodologies developed, and summarizes the results in graphical and tabular formats.

Volume II: Acceleration-Based Damage Detection, from the University of Iowa Center for Computer-Aided Design, presents the use of vibration-based damage-detection approaches as local methods to quantify damage at critical areas in structures. Acceleration data were collected and analyzed to evaluate the relationships between sensors and with changes in environmental conditions. A sacrificial specimen was investigated to verify the damage-detection capabilities and this volume presents a transmissibility concept and damage-detection algorithm that show potential to sense local changes in the dynamic stiffness between points across a joint of a real structure.

Volume III: Wireless Bridge Monitoring Hardware, from the University of Northern Iowa, Electrical Engineering Technology, summarizes the energy harvesting techniques and prototype development for a bridge monitoring system that uses wireless sensors. The functions and performance of the developed system, including strain data, energy harvesting capacity, and wireless transmission quality, are covered in this volume.

Integration of Bridge Damage Detection Concepts and Components
Volume II: Acceleration-Based Damage Detection

Final Report 2 of 3
October 2013

Principal Investigator
Brent M. Phares, Director
Bridge Engineering Center, Iowa State University

Co-Principal Investigators
Salam Rahmatalla, Associate Professor
Civil and Environmental Engineering, Center for Computer-Aided Design, University of Iowa

Jin Zhu, Associate Professor
Electrical Engineering Technology, University of Northern Iowa

Ping Lu, Rating Engineer
Office of Bridges and Structures, Iowa Department of Transportation

Research Assistant and Postdoctoral Scholar
Charles Schallhorn and Ghedhban Swadi

Authors
Salam Rahmatalla, Charles Schallhorn, and Ghedhban Swadi

Sponsored by
the Iowa Highway Research Board and Iowa Department of Transportation
(IHRB Project TR-636)

Preparation of this report was financed in part
through funds provided by the Iowa Department of Transportation
through its Research Management Agreement with the
Institute for Transportation
(InTrans Project 11-416)

A report from
Center for Computer-Aided Design
College of Engineering, University of Iowa
Iowa City, IA 52242
Phone: 319-335-5722

TABLE OF CONTENTS

ACKNOWLEDGMENTS ... vii
EXECUTIVE SUMMARY ... ix
Problem Statement ... ix
Objectives ... ix
Research Description and Key Findings ... ix
Implementation Readiness and Conclusions ... x
Implementation Benefits ... x
1. INTRODUCTION ... 1
1.1. Motivation ... 1
1.2. Background ... 2
1.3. Objective ... 3
2. THEORY ... 4
3. ALGORITHM ... 6
4. TESTING ... 10
4.1. Laboratory Testing ... 10
4.2. Field Testing (US 30 Bridge) ... 15
5. CONCLUSIONS AND RECOMMENDATIONS ... 28
REFERENCES ... 31
APPENDIX A. COHERENCE FOR ADDITIONAL PAIRS OF SENSORS FOR SACRIFICIAL SPECIMEN ... 33

LIST OF FIGURES

Figure 1. Outlined procedure for vibration-based damage-detection algorithm.............................6
Figure 2. Process outline for damage state comparison and warning percentage 8
Figure 3. Geometry and dimensions of connection specimen 10
Figure 4. Experimental layout of connection specimen..11
Figure 5. Connection specimen bolt removal plan: (a) damage scenario D0 (b) damage scenario D3 12
Figure 6. Coherence for pairs of sensors: (a) Sensors 2_1 (b) Sensors 2_3 13
Figure 7. Transmissibility diagrams of experimental connection specimen: (a) multiple damage scenarios at Nodes 2 and 1 (b) multiple damage scenarios at Nodes 2 and 3 14
Figure 8. Percent warnings of manual impacts for multiple damage states compared to baseline damage state for specimen connection 2_1 and 2_3..15
Figure 9. Typical time history of one-minute data file for traffic loading on bridge 16
Figure 10. Schematic layout of south span of US 30 bridge depicting locations of field experiments...17
Figure 11. Sensor orientation for Section C..17
Figure 12. Percent warnings for multiple days of traffic data compared to baseline day for Section C 18
Figure 13. Absolute differences in average daily temperatures from the baseline day for Section C 19
Figure 14. Sensor orientation for Section A 20
Figure 15. Percent warnings for multiple days of traffic data compared to baseline for sensors at Section A: (a) vertical sensors (b) horizontal sensors 21
Figure 16. Absolute differences in average daily temperatures from the baseline day for Section A..22
Figure 17. Sensor orientation for sacrificial specimen 23
Figure 18. Coherence for pair of Sensors 5 and 6...24
Figure 19. Percent warnings of manual impacts for multiple damage states compared to baseline damage state for the sacrificial specimen 25
Figure 20. Percent warnings of traffic data for multiple days compared to baseline day for the sacrificial specimen...26
Figure 21. Absolute differences in average daily temperatures from the baseline day for the sacrificial specimen..27

ACKNOWLEDGMENTS

The authors would like to thank the Iowa Highway Research Board (IHRB) and Iowa Department of Transportation (DOT) for sponsoring this research. The authors would also like the thank Ahmad Abu-Hawash and many other members of the Iowa DOT Office of Bridges and Structures for their continued support of this research.

EXECUTIVE SUMMARY

Problem Statement

Infrastructure health conditions and monitoring have been an active area of research and development due to the urgent demands for safer and longer-life structures. Many novel ideas have been developed and have shown success using simulations and lab testing, but have difficulties in detecting damage on large civil structures. The challenges are attributed to the complexity of these structures and the presence of noise and environmental effects/interferences.

Objectives

The objective of this part of the project was to validate/integrate a vibration-based damage-detection algorithm with the strain-based methodology formulated by the Iowa State University Bridge Engineering Center. The proposed algorithm for vibration-based measurements was based on localizing sensors around failure-critical joints and establishing transmissibility ratios. The methodology was tested using laboratory experiments and field testing.

Research Description and Key Findings

The vibration-based algorithm was tested and validated as follows:

- Laboratory experiments on a connection specimen using transient loading conditions
  - Warning percentages detected, quantified, and located damage
  - Percent warnings had difficulties in quantifying magnitudes of damage (could not exceed 100 percent)

- Field testing on a sacrificial specimen that was geometrically similar to the laboratory connection specimen
  - Warning percentages detected damage under normal traffic loading
  - Environmental effects (temperature, wind, construction, etc.) were believed to cause false damage results
  - Quantification of damage was unsuccessful due to variations caused by environmental effects

- Field testing of joints near the mid-span and quarter-span of a bridge girder
  - Warning percentages were utilized on bridge connections directly with substantial significance
  - False damage was detected when significant changes in temperature occurred and during construction of a trail under the bridge

Implementation Readiness and Conclusions

The transmissibility concept and damage-detection algorithm presented in this report demonstrate the potential to sense local changes in the dynamic stiffness between points across a joint of a real structure. Because the majority of failures occur at or near a connection, knowing the changes in inertial properties of failure-critical joints on a bridge would greatly improve detection capabilities and could prevent catastrophic failure.

This study showed that the presented algorithm is successful in experimental testing and that it has great potential for application in field analysis.

Further investigation is required to expand the understanding of how temperature affects warning percentages. Future work could entail temperature compensation within the damage-detection algorithm or provision of supplemental temperature information to add redundancy to the procedure.

Implementation Benefits

The validation and integration of the vibration-based and strain-based damage-detection methodologies will add significant value to Iowa’s current and future bridge maintenance, planning, and management.

1. INTRODUCTION

1.1. Motivation

With more than half of the 600,000 bridges in the US built before 1975, areas of research related to bridge maintenance, inspection, and monitoring have received significant attention in recent years (U.S. DOT 2012). Many of these bridges are classified as structurally deficient, and many other bridges that are considered fracture critical have the potential for catastrophic failure due to the lack of redundancy in the bridge design (Baker and Lowy 2013). All of the existing bridges, even those not in these damage-sensitive categories, could benefit significantly by implementing a near real-time damage-detection system with which the structural condition of the bridge can be monitored.

In general, the ideal damage-detection system would address all of the four damage issues in bridges (Rytter 1993): 1) detecting damage, 2) locating regions of damage, 3) quantifying the severity of damage, and 4) predicting remaining service life. Unfortunately, due to inevitable noise in field measurements, complicated boundary conditions, difficulty of measuring large structures with multiple materials, and potentially inadequate transducer sensitivity, even the most state-of-the art damage-detection methods struggle to provide insight into one or more of these issues when applied to civil infrastructure (Adewuyi et al. 2009, Chang et al. 2003).

In 2010, the University of Iowa completed a project for the Iowa Highway Research Board (TR-610) to develop a damage-detection tool based on vibration-based techniques. The work consisted of testing the effectiveness of using the changes in the frequency response functions of a structure as a means for damage detection. Toward this end, numerical simulations, laboratory experiments, and field testing were used.

While the results for the numerical simulations and lab testing have shown promise, the results of the field study were limited to information obtained from a healthy structure and were subjected to uncertainties in the operational loading and the complexity of the boundary conditions. The algorithm was, however, able to detect some differences in bearing conditions.

It appears that the frequency response function contains global information and therefore is not expected to detect local changes in the response of the structure unless it is used with a very fine mesh of sensors (Maia et al. 2011a, Johnson and Adams 2002). Another drawback of using the frequency response function in detecting damage in real structures is the complexity in measuring the operational input forces to the structure.

Research has been conducted showing the potential effectiveness of transmissibility in lieu of frequency response functions to detect damage within a system that is a local phenomenon (Maia et al. 2011a, Devriendt and Guillaume 2008). A localized damage-detection algorithm is presented in this work in which local information can be generated from the transmissibility function to identify local changes in joint stiffness of structures. In this case, damage is determined as any change in the structural response at selected locations around the joints.

It is proposed that by placing the sensors strategically at failure-critical locations and by having a reference sensor at a location where damage is unlikely to occur, it could be possible to detect, locate, and quantify damage accurately for an entire structure utilizing localized damage-detection principles.

1.2. Background

Local damage-detection techniques, such as acoustic approaches (i.e., ultrasonic, impact-echo, tap test) and visual approaches (i.e., x-ray and gamma ray), have been proven to detect damage accurately in the region very close to where the technology is deployed (Guo et al. 2005). However, the logistics and cost associated with using these methods on civil infrastructures can outweigh the benefits even for relatively small structures (Chang et al. 2003, Guo et al. 2005).

The concept of vibration-based damage-detection methods is that a change in dynamic characteristics (mass, stiffness, or damping) can be detected by observing the associated change in modal parameters such as natural frequency, mode shape, frequency response function (FRF), and transmissibility (TR).

Although many methods have been investigated, few have shown success in field implementation (Doebling et al. 1996), mainly due to the environmental effects (i.e., temperature, wind) (Chesne and Deraemaeker 2013). Works completed by Maia et al. (2001), Maia et al. (2011b), and Weijtjens et al. (2013) show theoretically that transmissibility can be used for more accurate and sensitive localized damage detection than frequency response functions or mode shapes. These properties of transmissibility are discussed in Chapter 2.

Vibration-based damage-detection algorithms generally consist of placing numerous sensors to obtain a global response to a structural system. Damage is then determined as any change in the global response when compared to that from another time period. Again, it is proposed that by placing the sensors strategically at failure-critical locations and by having a reference sensor at a location where damage is unlikely to occur, it could be possible to detect, locate, and quantify damage accurately for an entire structure utilizing localized damage-detection principles.

The main concept of the proposed algorithm comes from an understanding of acceleration-based sensors and how the proximity from damage affects the signal collected by the sensor. Acceleration-based sensors are expected to be sensitive to both the global and the local responses of a system. If any damage is introduced into the system, the sensor should be able to detect the changes in the dynamic response compared to the dynamic response from a previous time point. The local response of the system would have a much larger effect on the signal and, therefore, insight into damage location and quantification can be determined by the proximity of the damage to the sensor.

1.3. Objective

For the vibration-based algorithm presented here, the theme is to show that vibration-based damage-detection approaches are heavily investigated as global methods; however, little work has been done to investigate their effectiveness as local damage-detection schemes, especially for field applications.

The objective of this study is to use vibration-based damage-detection approaches as local methods to quantify damage at critical areas in structures. Acceleration data were collected and analyzed to evaluate the relationships between sensors and with changes in environmental conditions. A sacrificial specimen was investigated to verify the damage-detection capabilities.

2. THEORY

The dynamic response of a structure is described as the influence or motion of the system due to a non-static loading, such as an impulse load or forced vibration. Generally, the dynamic response is a measure of the vibration of the system. Equations of motion have been commonly used to solve for the displacements, velocities, and accelerations at determined locations, thus resulting in the motion of a system due to an applied force. The equation of motion for a general system is shown in Equation 1, where M is the mass matrix of the system, C is the damping matrix, K is the stiffness matrix, $\ddot{u}(t)$ is the nodal acceleration vector, $\dot{u}(t)$ is the nodal velocity vector, $u(t)$ is the nodal displacement vector, and F(t) is the applied force vector.

$$\mathrm{M}\ddot{u}(t) + \mathrm{C}\dot{u}(t) + \mathrm{K}u(t) = F(t) \quad \textbf{(1)}$$

In theory, the mass, damping, and stiffness matrices, as well as the applied force vector, are all known quantities, therefore, Equation 1 is used to solve for the nodal displacements and their time derivatives. Once these values are determined, the acceleration can be transformed from the time domain to the frequency domain by applying a Fourier transform. Changes in the response of the system can be seen in the time domain; however, they can be seen more easily in the frequency domain as changes in the natural frequencies and mode shapes of the system.

For a single applied force, Equation 1 can be transformed to the frequency domain:

$$\mathrm{D}(s)u(s) = F(s) \quad \textbf{(2)}$$

where D is the dynamic stiffness of the structure. For an undamped system, D can be represented as:

$$\mathrm{D} = \mathrm{K} - \omega^2\mathrm{M} \quad \textbf{(3)}$$

where K represents the stiffness of the structure, M is the structure's mass, and ω is the natural frequency of the structure. Equation 2 can also be written as:

$$u(s) = \mathrm{H}(s)F(s) \quad \textbf{(4)}$$

where H(s) is the inverse or pseudo-inverse of the dynamic stiffness matrix D, which is also called the frequency response matrix, and can be calculated using the H_1, H_2, or H_v approaches (Ewins 2000):

$$\mathrm{H}_1(\omega) = \frac{S_{fx}}{S_{ff}} \quad \textbf{(5)}$$

where S_{fx} is the cross-spectral density between the input force and the output displacement, and S_{ff} is the auto-spectral density of the input force on the system.

$$H_2(\omega) = \frac{S_{fxx}}{S_{xf}} \quad \textbf{(6)}$$

For noisy data, the FRF can be calculated using the following function:

$$H_V(\omega) = \sqrt{H_1(\omega)H_2(\omega)} \quad \textbf{(7)}$$

The transmissibility (T^k_{ij}) between two locations (i and j) on a structure as a result of an applied force at location (k) can be defined as the ratio between the frequency response functions $H_{ik}(\omega)$ and $H_{jk}(\omega)$:

$$T^k_{ij}(\omega) = \frac{H_{ik}(\omega)}{H_{jk}(\omega)} \quad \textbf{(8)}$$

The transmissibility can also be defined directly from output-only responses, which is common when examining a system where H cannot be determined. The ratio between the response at position X_i and X_j directly gives the same relationship as Equation 8:

$$T^k_{ij}(\omega) = \frac{X^k_i(\omega)}{X^k_j(\omega)} = \frac{H_{ik}(\omega)}{H_{jk}(\omega)} \quad \textbf{(9)}$$

While it relates the motion information from two locations, the transmissibility function is expected to be more sensitive to local changes when compared with the frequency response function (H).

Ribeiro et al. (2000) similarly derived a general formulation of transmissibility. In the formulation, it is defined that $\{F\}$ is a vector of applied forces, $\{X_U\}$ is a vector of unknown responses, $\{X_K\}$ is a vector of known responses, and [H] is the FRF matrix for the structure. Similar to Equation 4, the relation between the applied forces and a set of responses is given by:

$$[H_{KA}]\{F_A\} = \{X_K\} \quad \textbf{(10)}$$

$$[H_{UA}]\{F_A\} = \{X_U\} \quad \textbf{(11)}$$

where $[H_{KA}]$ is the sub-matrix of [H] relating the known responses to the applied forces and $[H_{UA}]$ is the sub-matrix of [H] relating the unknown responses to the applied forces. If $[H_{KA}]$ can be inverted (e.g., $\#K \geq \#A$), the following relationship is possible:

$$\{X_U\} = [H_{UA}][H_{KA}]^{-1}\{X_K\} = [T^A_{KU}]\{X_K\} \quad \textbf{(12)}$$

where $[T^A_{KU}]$ is the transmissibility matrix between the sets of coordinates K and U when the forces are applied at coordinates A.

3. ALGORITHM

In this chapter, the vibration-based damage-detection algorithm developed for integration with the Iowa State University (ISU) Bridge Engineering Center (BEC) damage-detection methodology is presented. This procedure incorporates many characteristics similar to the processes described previously, while adding novel aspects to data collection and analysis in pursuit of an accurate localized vibration-based damage-detection algorithm that can be implemented in field environments. The procedure is outlined in Figure 1.

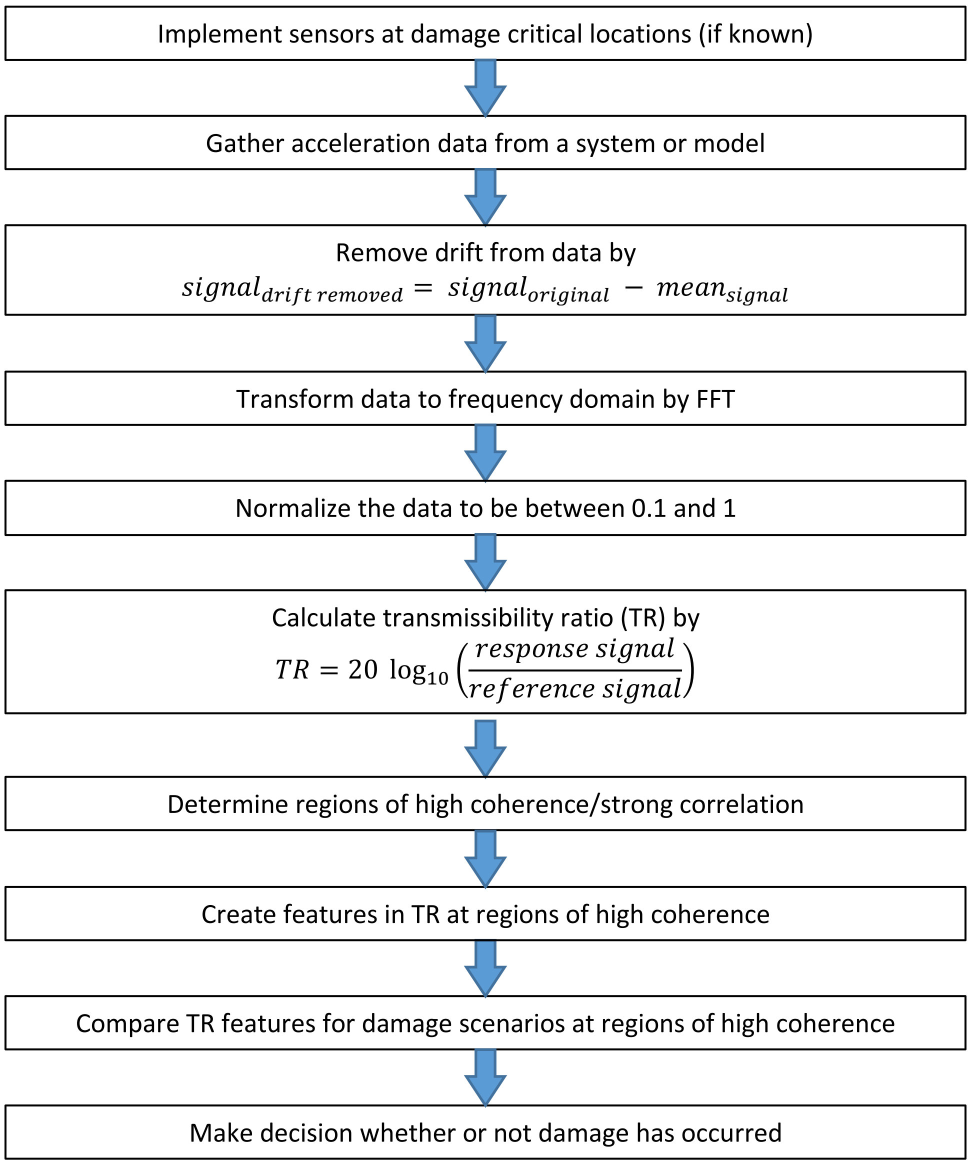

Figure 1. Outlined procedure for vibration-based damage-detection algorithm

The algorithm begins with the proper installation of sensors. Throughout this project, piezoelectric accelerometers were used for data collection. With an understanding of the dynamics of the structure to measure, sensors could be placed at or near damage-critical locations (i.e., connections, high-stress areas). Placing the sensors around these damage-critical locations directly localizes the scope of the detection algorithm, thus improving the likelihood of detecting small deficiencies.

With the sensors implemented in optimal locations, data could then be collected for any loading scenario. Two types of loading scenarios were used in this project for analysis: transient (impacts) and ambient (traffic). Depending on which loading scenario was applied, the data points used for damage state sets within the algorithm were calculated differently. Individual impacts were used from transient loading, and specified durations of the time history responses (one-minute files) were used for ambient loading.

Depending on environmental conditions, sensor type, and other factors, drift may occur during data collection and must be removed accordingly. Drift is removed by subtracting the mean value from the original signal. It is most accurate when this calculation is carried out on a series of small time steps per time history file (Phares et al. 2011).

The data is then transformed to the frequency domain using a fast-Fourier transform (FFT). Given that the loadings will not be exactly the same experimentally, data normalization is used such that an accurate representation of the transmissibility ratio (TR) can be determined. Without this normalization, the ratio of the response signal to the reference signal could be distorted based on loading conditions alone. Once the signals are normalized, the TR is calculated by using the equation in Figure 1 above, where the log of the ratio is multiplied by 20, making dB the units for TR.

The decision process for detecting damage is based on changes to the TR for a given pair of sensors. Similar to the work completed by Maia et al. (2011a), the damage decision can be calculated by discretizing the TR as a collection of features in which each feature is a range of frequencies. It has been proposed that it is possible to investigate the effect of damage only on certain frequency bands (Schulz et al. 1997), and Chesne and Deraemaeker (2013) state that it is possible to increase the accuracy of the decision process by limiting these features. It is proposed to look at the coherence between sensor signals to limit these features.

After obtaining the regions of high coherence, the comparison between damage states can be conducted to decide if damage can be detected. The decision for detection is calculated as a warning percentage for each set of data points. For purposes of clarification, two sets of data are referred to in the discussion of the proposed algorithm: baseline set and comparison set. The baseline set is comprised of all of the data (TR between pairs of sensors) collected for the healthy or undamaged state and the comparison set is all of the data collected for a single damaged state. There can be many comparison sets per analysis, but only one baseline set.

The warning percentage is an indication of the percent of data points (impacts or one-minute files) in a given set that are statistically different from the baseline set of data points and difference from the baseline set is classified as damage.

The calculation to determine if a point is statistically different from the baseline set is shown in Figure 2.

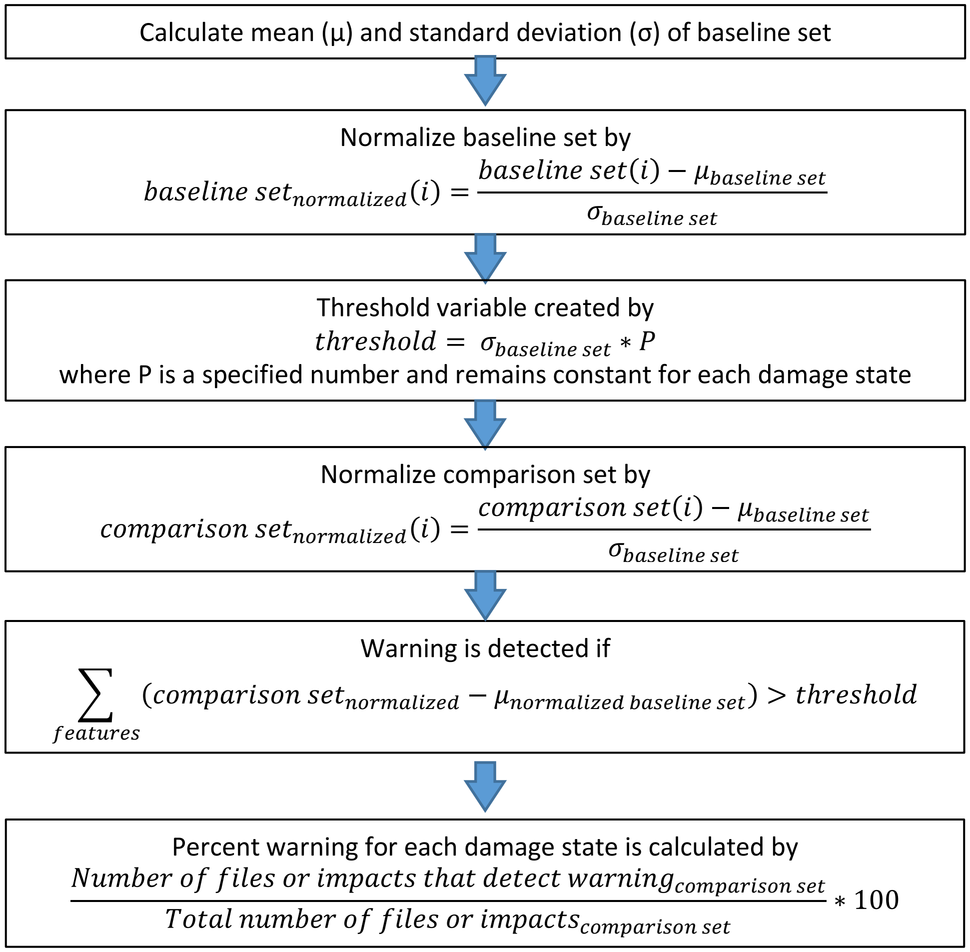

Figure 2. Process outline for damage state comparison and warning percentage

The mean and standard deviation of the baseline set of TR for a given pair of sensors are calculated and used to normalize the baseline set. This normalization is completed to account for the magnitude differences of the TR for each feature (frequency range). A threshold variable is created to allow a buffer between data points. This buffer accounts for the variations in TR due to noise, environmental conditions, etc. The comparison data are then normalized by the same parameters as the baseline set normalization.

By utilizing the regions of high coherence, the ranges of frequencies (features) are used to discretize the sets of normalized data. For each feature, the difference between the normalized comparison set and the mean of the normalized baseline set is calculated, thus returning a vector of values for each feature. The summation of these values for the length of the vector is compared with the threshold variable to determine if a warning is detected for the impact or one-minute file.

Collecting these warnings for multiple impacts or files leads to the warning percentage, which give a more accurate representation of the damage state. These warning percentages are proposed to not only detect damage, but to also offer quantification between damage states.

4. TESTING

4.1. Laboratory Testing

4.1.1. Equipment

Laboratory testing was conducted on a specimen, geometrically simulating the girder-floor beam connections, to investigate the structural behavior mimicking that seen in a bridge connection. This specimen is referred to as the connection specimen. The dimensions and layout of the specimen are shown in Figure 3.

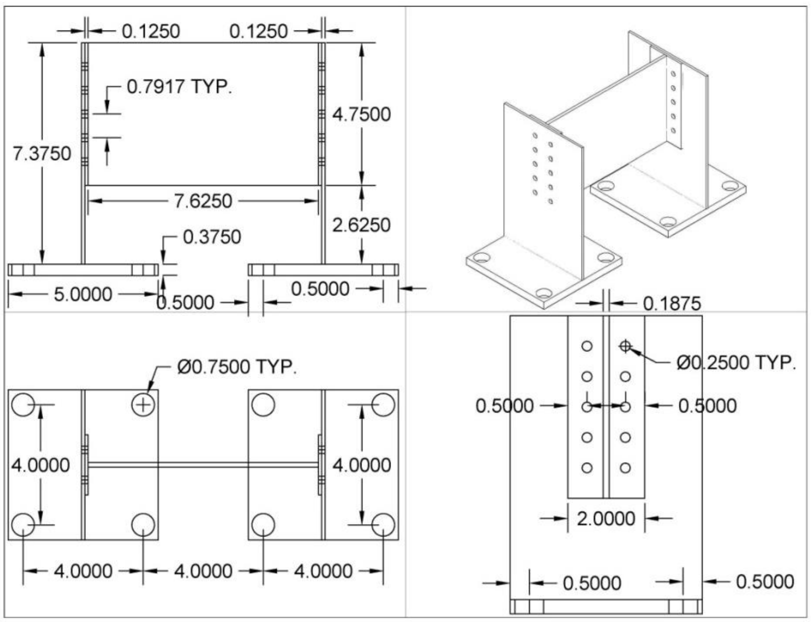

Figure 3. Geometry and dimensions of connection specimen

The connection specimen was constructed out of general steel and the dimensions were slightly modified from a 1/4 scale representation of the sacrificial specimen used in previous work completed by ISU (Phares et al. 2011). Bolted connections were chosen over welded connections to allow for repetition of experiments and to provide the option for different damage scenarios to occur without sacrificing the specimen.

The connection specimen was mounted on top of pieces of high-density rubber to minimize the effects of external vibrations, and a total of 20 steel bolts (10 at each connection) were used to connect the three portions of the specimen. Two 100 g range Dytran triaxial accelerometers and one 100 g range Dytran uniaxial accelerometer were fixed to the structure by attaching a magnetic base and then gluing the magnetic base to the specimen.

The axis of interest for this experiment was parallel to that of the longest dimension of the middle portion of the connection specimen. A 500 lb F limit Dytran impulse hammer was used as the excitation for the transient analysis, and a DEWE-43 data acquisition system was used to obtain the data.

For all of the damage scenarios, a sampling rate of 5,000 samples per second was used. All of the programs required for the damage-detection algorithm were written in MATLAB, in which the data gathered by the DEWE-43 system was easily converted to the appropriate file format for use.

4.1.2. Connection Specimen

An illustration of the connection specimen, sensor location, and impact location is shown in Figure 4. Note that the location of Sensor 3 is symmetrically identical to that of Sensor 1.

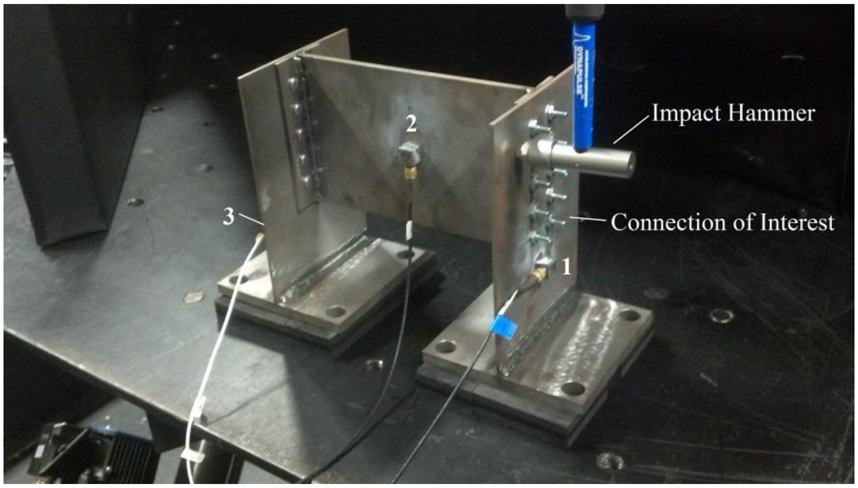

Figure 4. Experimental layout of connection specimen

4.1.3. Placement of Accelerometers and Location of Impact

Acceleration data was gathered from all sensors for a series of 20 impacts, in which each impact could be used for a transient analysis (i.e., the motion of the connection specimen damped to zero before the next impact). Each series of 20 impacts created a set of data for a given damage state and a seven damage severities were analyzed (0, 1, 2, 3, 4, 5, and 6 bolts removed). The damage was introduced by successively removing one bolt from the connection of interest (between Sensors 1 and 2 only). The pattern for which bolts were removed is shown in Figure 5.

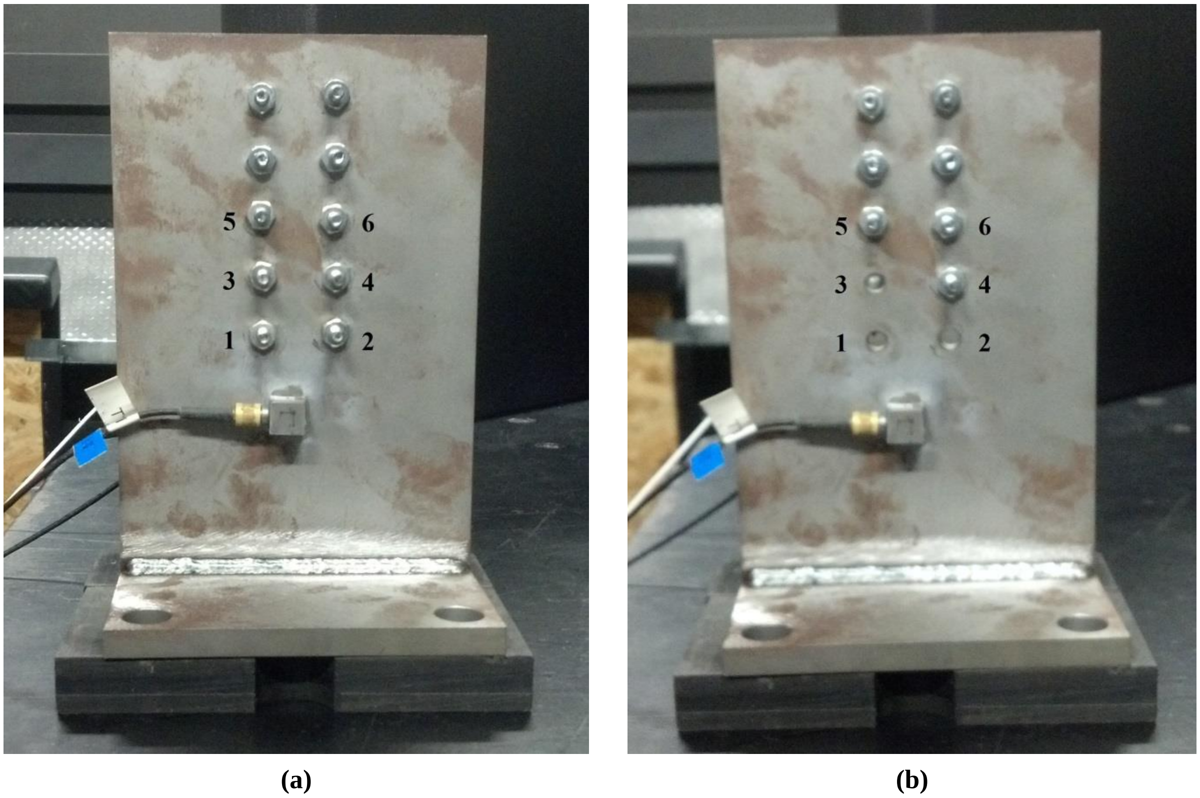

Figure 5. Connection specimen bolt removal plan: (a) damage scenario D0 (b) damage scenario D3

The data acquired for this experiment was then used to calculate the TR for symmetric sides of the connection specimen (i.e., the TR between Sensors 1 and 2 and between Sensors 2 and 3). The notation for each damage scenario is D#_Ref_Res, where # is the number of bolts removed, Ref refers to the reference node, and Res refers to the response node. For example, D2_2_1 corresponds to the damage scenario with 2 bolts removed, with Node 2 as the reference signal and Node 1 as the response signal. The coherence is shown in Figure 6, and the regions of high coherence used for the analysis was decided as the ranges from 30 to 215 Hertz and 325 to 410 Hertz. The averaged TR over 20 impacts of Nodes 1, 2, and 3 for each damage scenario is shown in Figure 7.

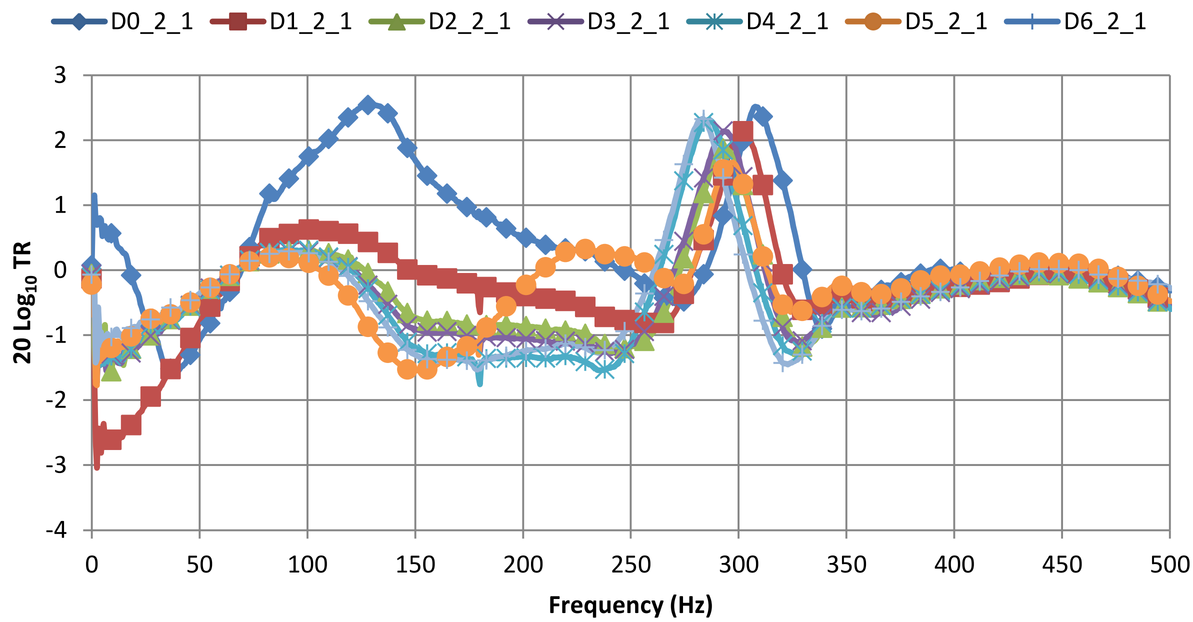

(a)

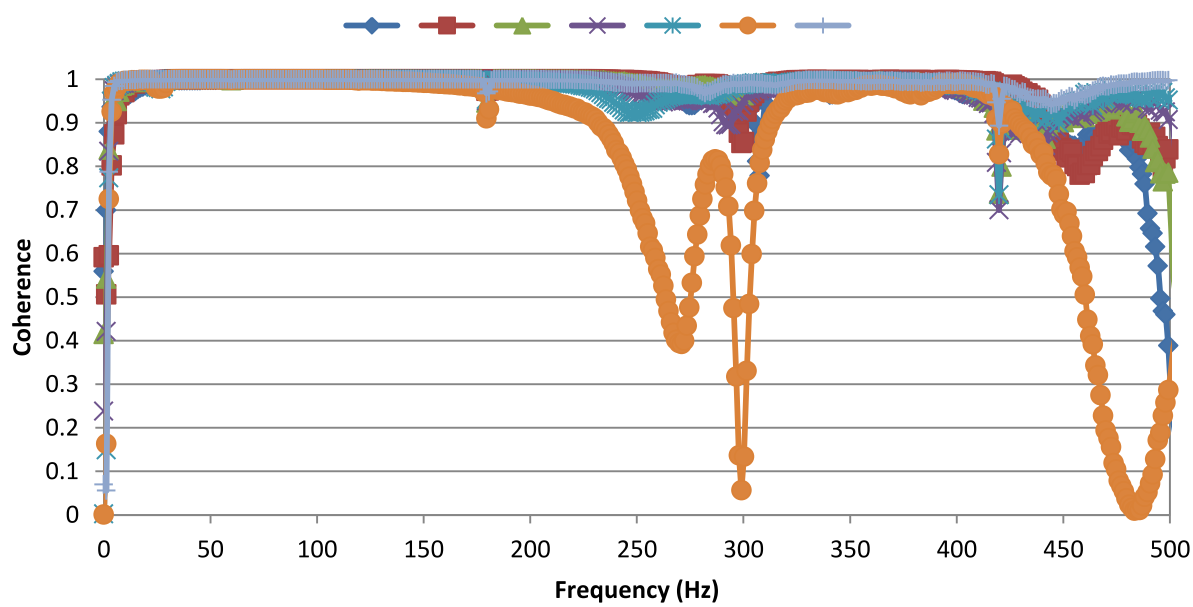

(b)

Figure 6. Coherence for pairs of sensors: (a) Sensors 2_1 (b) Sensors 2_3

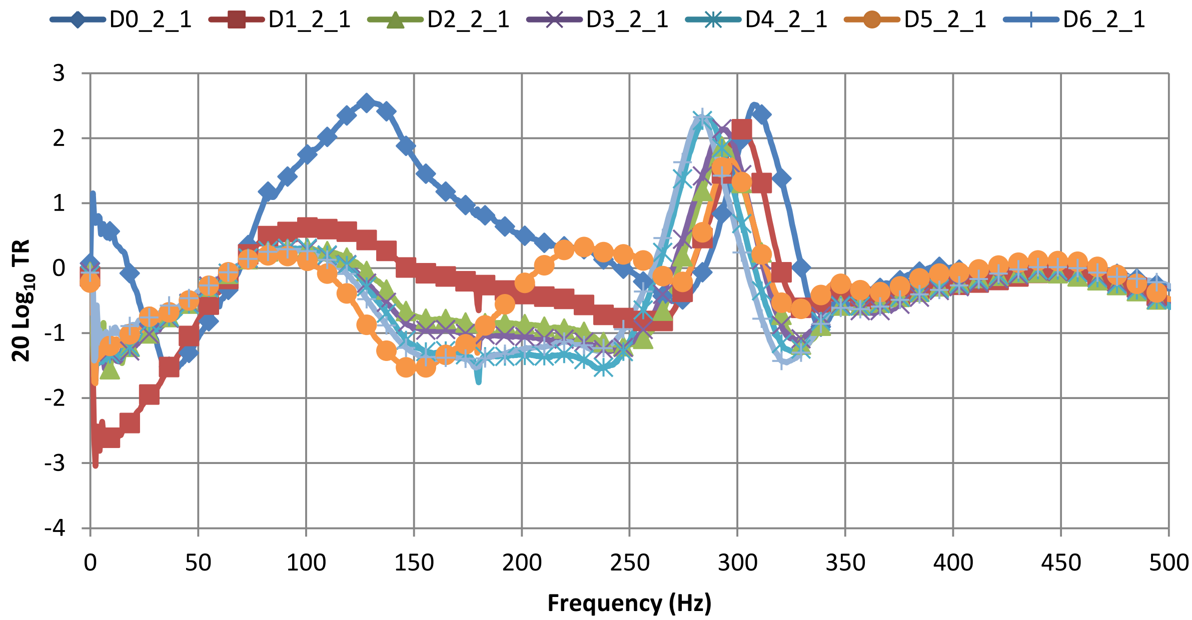

(a)

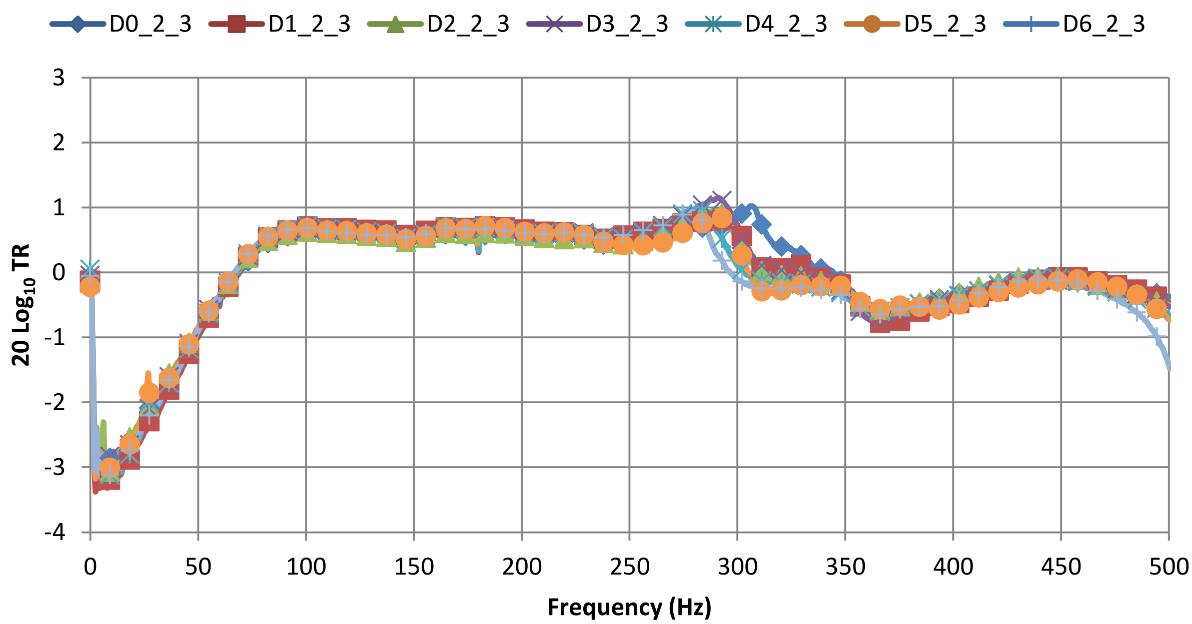

(b)

Figure 7. Transmissibility diagrams of experimental connection specimen: (a) multiple damage scenarios at Nodes 2 and 1 (b) multiple damage scenarios at Nodes 2 and 3

It is apparent that the damage caused by removing bolts in a connection changes the transmissibility between sensors adjacent to the damage significantly, while the transmissibility between sensors away from the damage are nearly unaffected. Given that damage is clearly detected and located for these pairs of transmissibility, the feature extraction algorithm was used for validation. The percent warning for each damage state is shown in Figure 8.

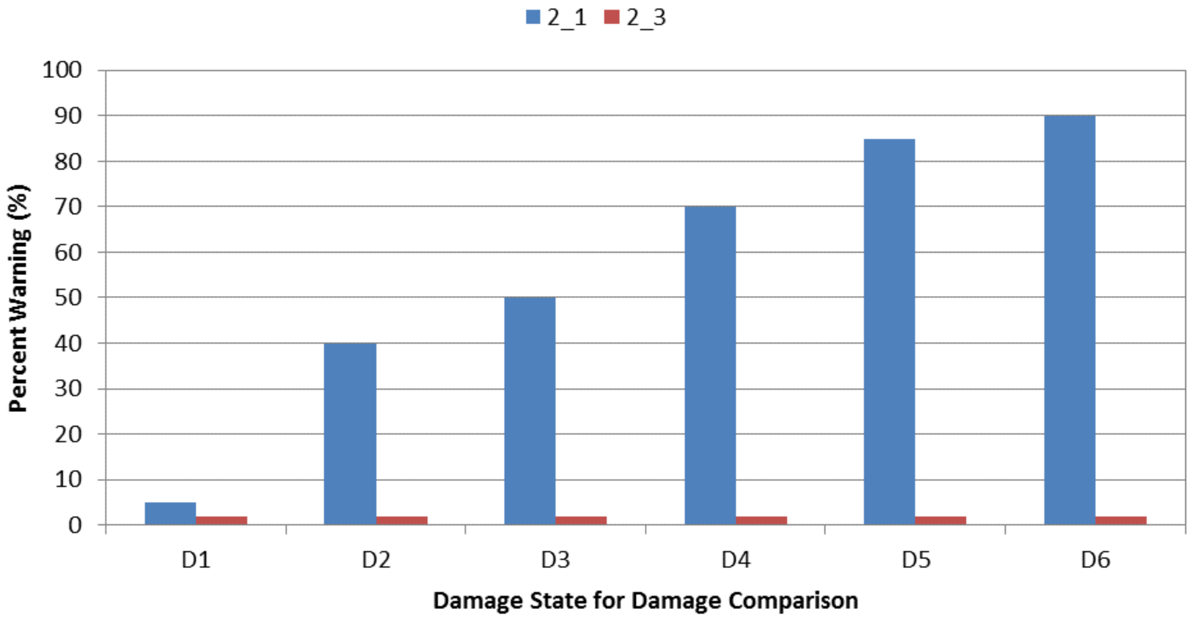

See Figure 4 for sensor locations

Figure 8. Percent warnings of manual impacts for multiple damage states compared to baseline damage state for specimen connection 2_1 and 2_3

The feature extraction algorithm clearly identifies damage between Sensors 1 and 2 (tall blue bars in Figure 8) for all damage scenarios and quantification of damage is seen by the increasing warning percentage. No damage is detected between Sensors 2 and 3 (short red bars in Figure 8), which is expected given that the properties of transmissibility allow for local detection. Based on the results from this experiment, the algorithm shows great potential for detecting, quantifying, and locating damage within a system.

4.2. Field Testing (US 30 Bridge)

4.2.1. Equipment

To implement the presented algorithm in the field, a variety of equipment and materials were utilized to obtain the dynamic characteristics of the bridge. The data acquisition system was constructed by ISU, in which six additional sensor adaptors were installed to account for the accelerometers to be implemented on-site. Six Brüel and Kjaer 0.5 g range DeltaTron uniaxial seismic accelerometers were used for a better signal-to-noise ratio, as well as to increase the sensitivity of the damage-detection capabilities significantly.

Each sensor was attached to a base plate or bracket (for directionality purposes, and an L-bracket was used in some locations) and the base was then epoxied to the structure. To protect the sensor from the environment, and in case of detachment, each sensor was wrapped in plastic wrap, foam strips, and duct tape. For some sensors, spray-on foam insulation was used around the base to help weatherize the sensor.

Data files consisting of one-minute intervals of traffic data for all sensors were transmitted to the University of Iowa (UI) via a secure file transfer protocol (ftp) site hosted by ISU, allowing for remote access to and usage of the data. A typical data file for acceleration is shown in Figure 9.

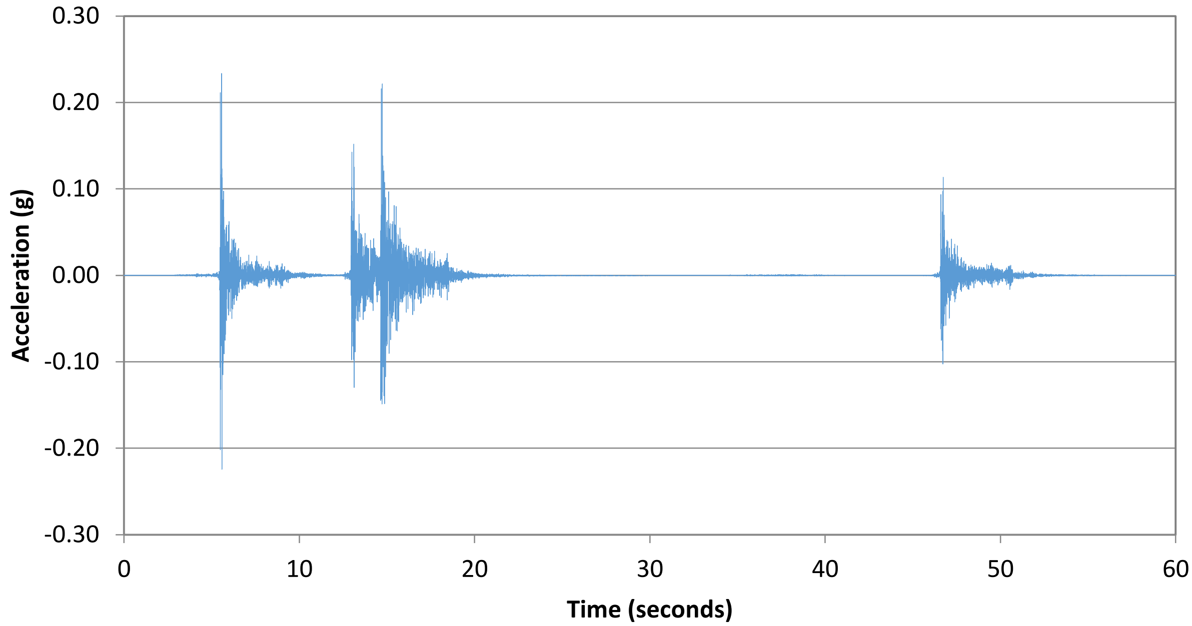

Figure 9. Typical time history of one-minute data file for traffic loading on bridge

Each one-minute files was then compiled (by day or 1,440 files) in MATLAB to then be used in the presented algorithm, which was written as a series of MATLAB programs. A total of 35 days of data, non-consecutive, were used for the analysis of Section C (Figures 10 and 11) and the sacrificial specimen (Figure 17) starting on September 13, 2012 and ending on November 6, 2012. Thirty-eight days of data, non-consecutive, were used for the analysis of Section A (Figures 10 and 14) beginning on November 27, 2012 and ending on March 11, 2013.

All of the field experiments for this project were conducted under the south span of the US 30 Bridge. A schematic of the bridge and the experiment locations are shown in Figure 10.

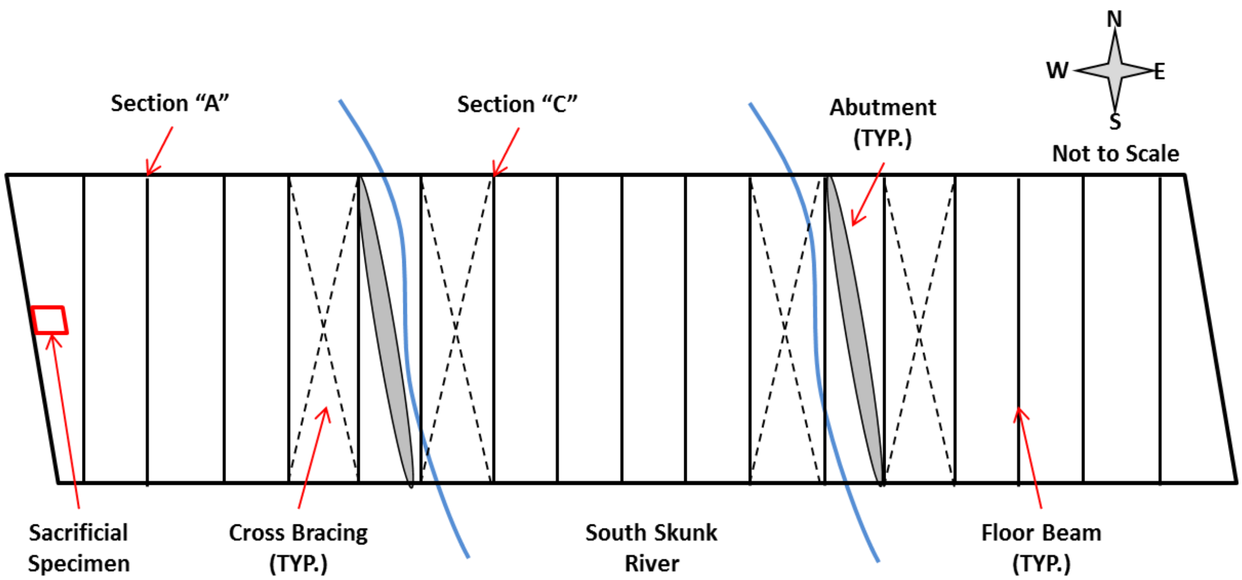

Figure 10. Schematic layout of south span of US 30 bridge depicting locations of field experiments

4.2.2. Section C

Data were collected for a beam-girder connection at Section C, shown in Figure 11.

Figure 11. Sensor orientation for Section C

The purpose of this data acquisition and analysis was to demonstrate the likelihood of false damage detection, as no damage was created intentionally at this joint, and damage was not expected to occur throughout the duration of the project.

Following the same procedure as the connection specimen (Section 4.1.2), the acceleration data from the traffic vibrations were used to determine the TR between the pair of sensors shown above.

In lieu of having damage states for comparison, each day of data (set of 1,440 one-minute files) was used for comparison, and a warning percentage was calculated based on these evaluations. To account for some of the noise and nonlinearity of the system, a buffer was introduced such that percentages less than the buffer limit (10 percent) were still considered acceptable or non-damaged. As shown in Figure 12, false damages were detected for a few days near October 10 and all of the days after October 27.

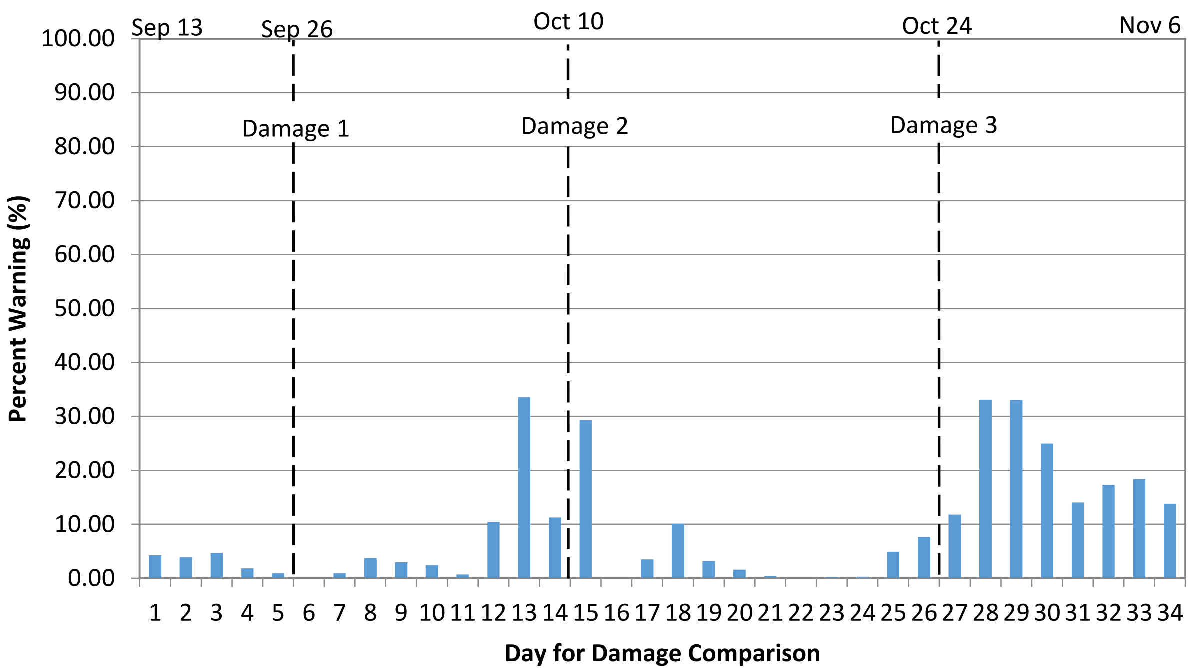

See Figure 11 for sensor locations

Figure 12. Percent warnings for multiple days of traffic data compared to baseline day for Section C

The dashed vertical lines and damage labels refer to the days when damage was created in the sacrificial specimen, which is discussed later. Initial investigation of the false damages showed an association between percent warning and temperature. The temperature is averaged over the same 24 hour period for the comparison to the baseline data, and each comparison day's average temperature is shown in Figure 13.

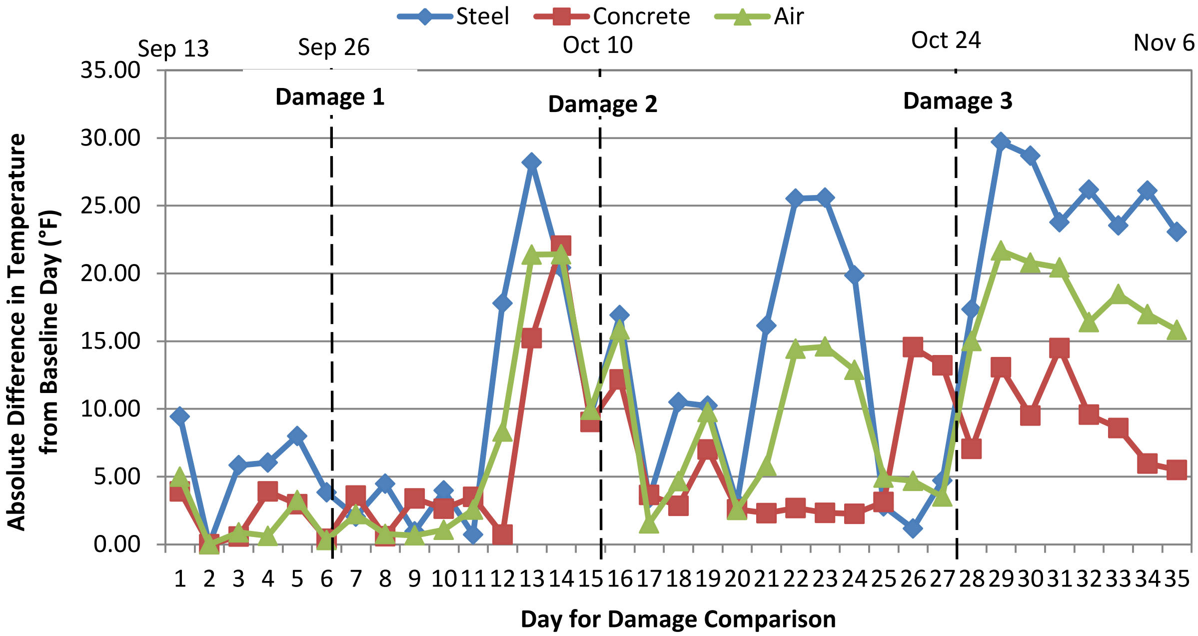

Figure 13. Absolute differences in average daily temperatures from the baseline day for Section C

When comparing the percent warnings for Section C with the absolute differences in temperature for these days, it's apparent that these false damage warnings occur during significant changes in temperature. The exception to this, and the justification for further investigation, is the significant change in temperature between October 10 and October 27 that did not alter the percent warning significantly.

The association between percent warning and temperature changes suggests that for any significant change in temperature between days (or during the same day), a similarly significant change occurs within the warning percentage. Further investigation is required to better understand the relationship between temperature and damage quantification. Overall, the presented algorithm was successful at detecting damage for days in which temperatures remained near stationary; therefore, this algorithm could benefit from supplementary temperature information to negate false warnings.

4.2.3. Section A

Similar to Section C, data were collected at Section A to investigate the likelihood of false warnings, as well as explore temperature effects and sensor orientation. Due to the complexity and nonlinearity of the loading and response of the bridge, a parametric study was completed to determine the ideal orientation of the sensors. The layout and labels of each of the sensors used for this study are shown in Figure 14. The odd-numbered sensors were vertical and the even-numbered sensors were normal to the web of the north girder.

Figure 14. Sensor orientation for Section A

In a similar fashion to that of Section C, the data were analyzed for Section A and about a month of data were usable. The warning percentages, as compared to the baseline day (November 27, 2012) are shown in Figure 15. From all of these relationships, the vertical sensors give cleaner results and therefore validate the orientation of the sensors in the previous studies.

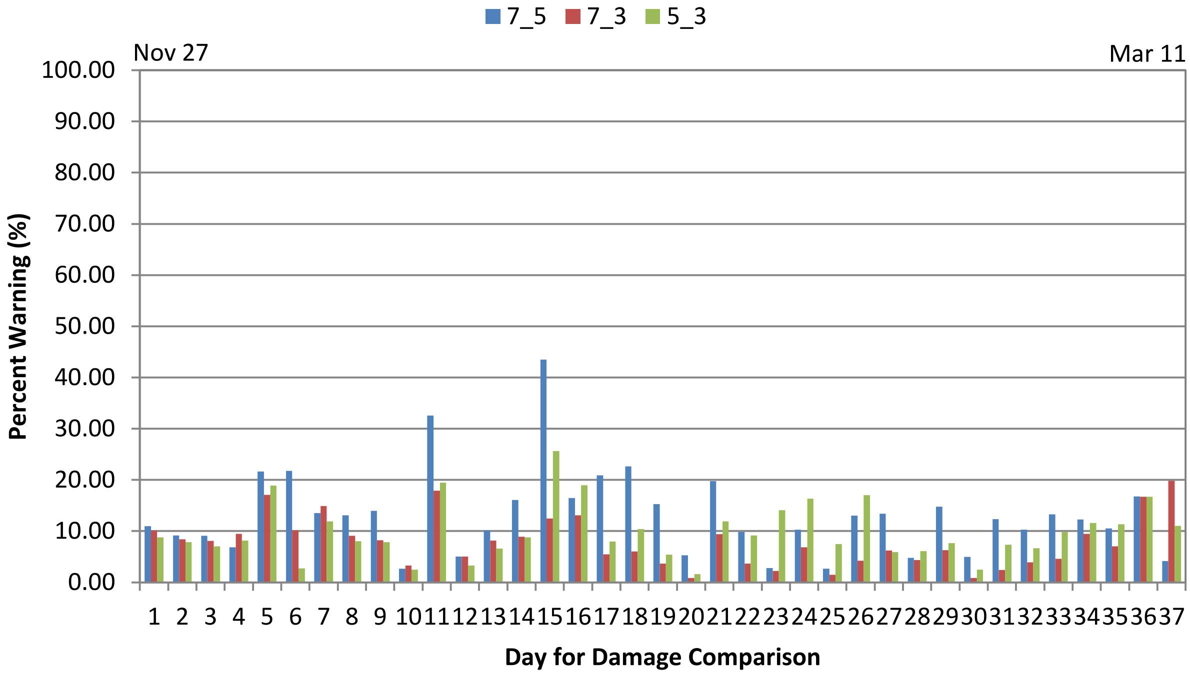

(a)

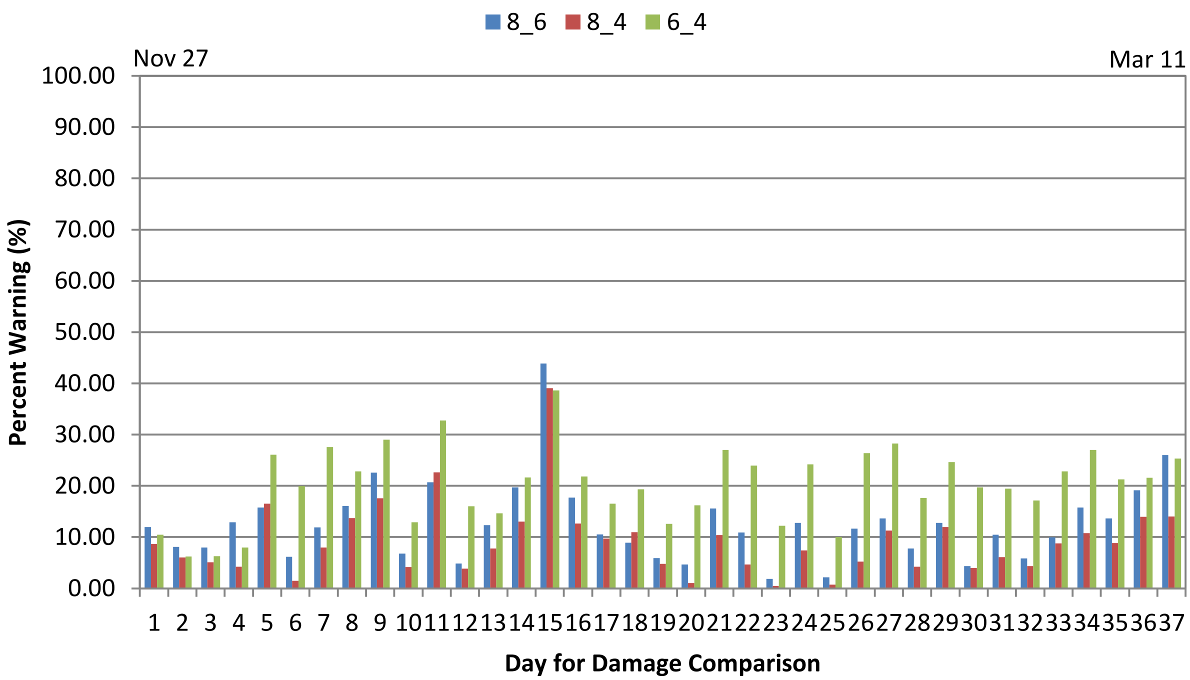

(b)

See Figure 14 for sensor locations

Figure 15. Percent warnings for multiple days of traffic data compared to baseline for sensors at Section A: (a) vertical sensors (b) horizontal sensors

Temperature effects were also investigated, and, similar to Section C, false damage detection could be related to significant changes in temperature. When comparing Figure 16 to the warning percentages, some of the false damages are related to significant changes in temperature, while others are not. Therefore, further investigation is needed to understand the temperature effect on this damage-detection algorithm.

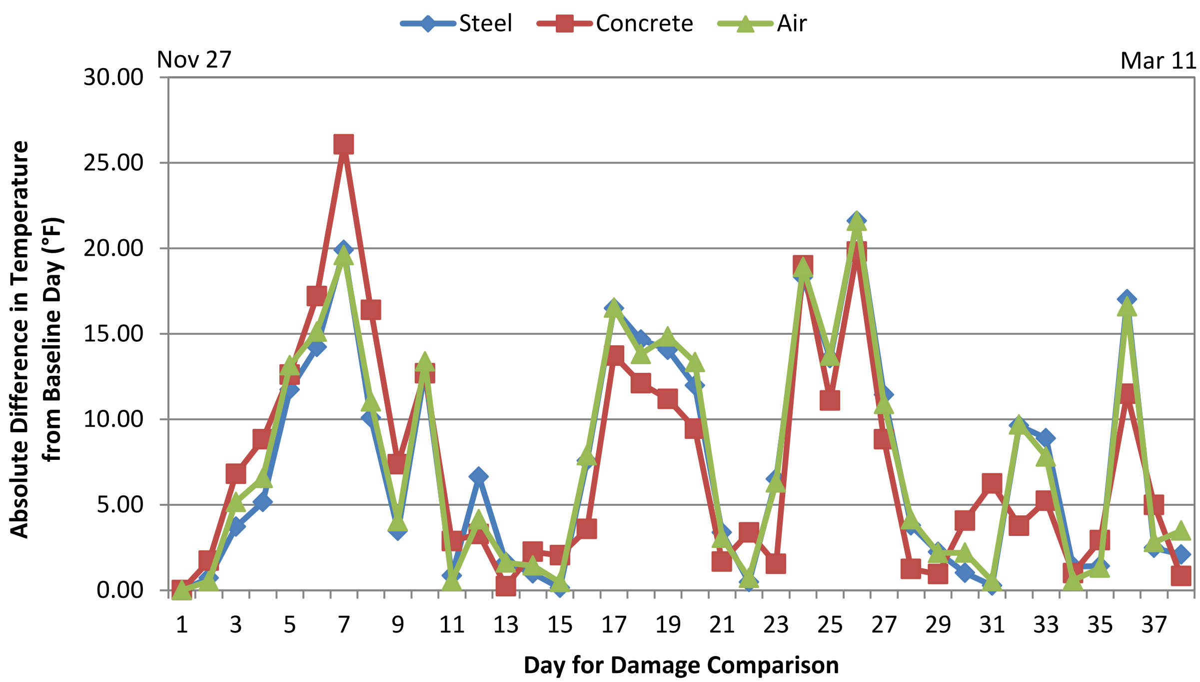

Figure 16. Absolute differences in average daily temperatures from the baseline day for Section A

Overall, damage is clearly detected for days when the temperature remained stationary. Therefore, this algorithm is proving successful in field applications.

4.2.4. Sacrificial Specimen

To further validate the presented algorithm in field testing, the sacrificial specimen (Phares et al. 2011) was utilized to determine if fatigue cracks could be detected through normal traffic loading. The sacrificial specimen used for this work is shown in Figure 17, as are the labels and locations of the accelerometers implemented on the specimen.

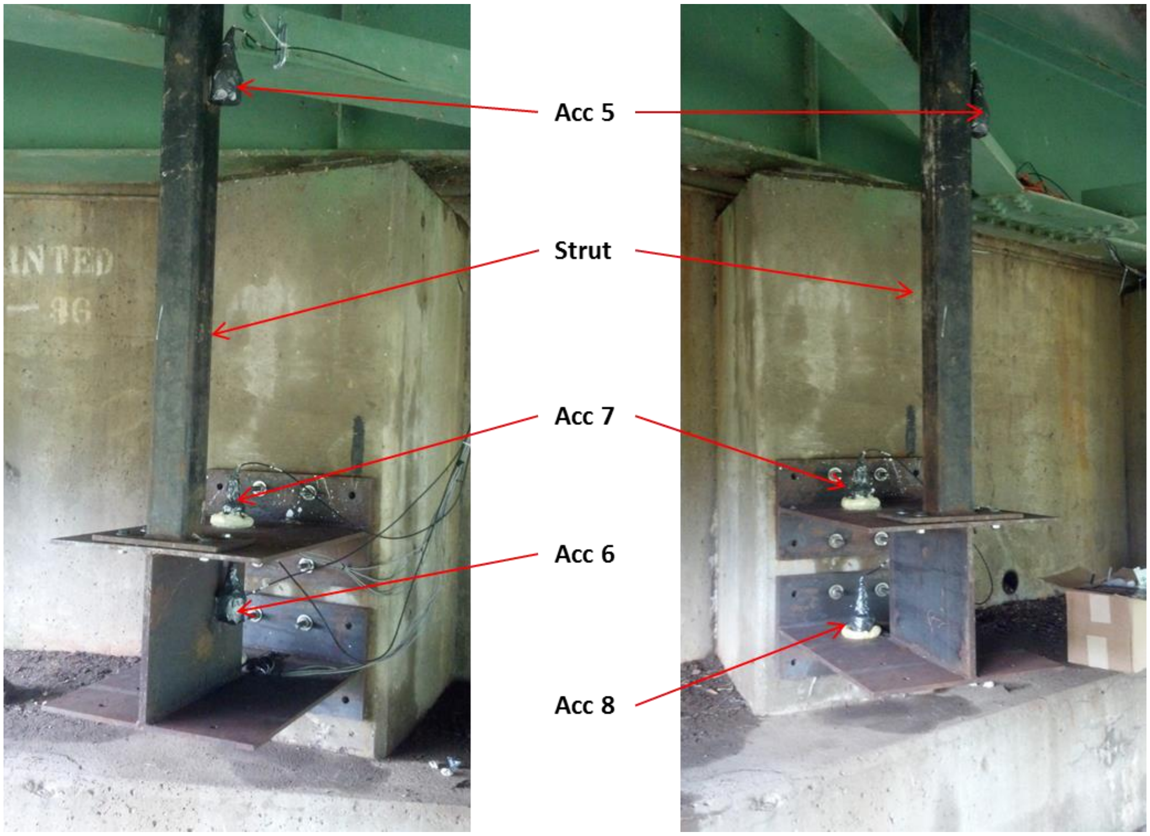

Figure 17. Sensor orientation for sacrificial specimen

All of the sensors were installed to measure vertical acceleration due to the loading being transmitted vertically to the specimen from the bridge via the strut. The direction that had the largest motion was vertical; therefore, the signal strength in the vertical direction was optimal. As traffic crossed the bridge, the vibration of the girders would be transferred to the sacrificial specimen via the strut.

These vibrations were captured by the sensors implemented on the specimen and then transmitted to UI for analysis. As the decision process dictates, a percent warning for each day was determined to ascertain how different the compared signals were from the baseline. To account for some of the noise and nonlinearity of the system, a buffer was introduced such that percentages less than the buffer limit (10 percent) were still considered acceptable or non-damaged.

Data were collected for two weeks for the undamaged sacrificial specimen to create a baseline set. Of these two weeks of data, one day (24 hour period from midnight to midnight) was designated as the baseline day (September 14, 2012), with which all other days of data were compared. After the initial two weeks of data collection, damage was introduced into the sacrificial specimen by an accelerated fatigue method. This process included removing the strut (so as to not cause damage to the bridge), placing a shaker on the specimen, vibrating the specimen at its natural frequency until a fatigue crack initiates or propagates a certain amount, and then replacing the strut.

An additional two weeks of data were collected for this damage state, and then damage was propagated again. This cycle continued until three damage states were completed and eight weeks of data were collected.

On the days when damage was created or propagated, a transient analysis was conducted on the sacrificial specimen without the strut attached to investigate any effect the removal and replacement of the strut might have on the damage-detection process. These transient analyses were conducted by impacting the specimen with the hammer used in the laboratory tests.

Each test consisted of approximately 50 impacts to obtain statistical significance. Two tests were conducted on the same day that damage was created: one before the damage and one after the damage. Figure 18 shows the coherence between Sensors 5 and 6, and the regions of high coherence used for the analysis was set as the range from 15 to 35 Hertz.

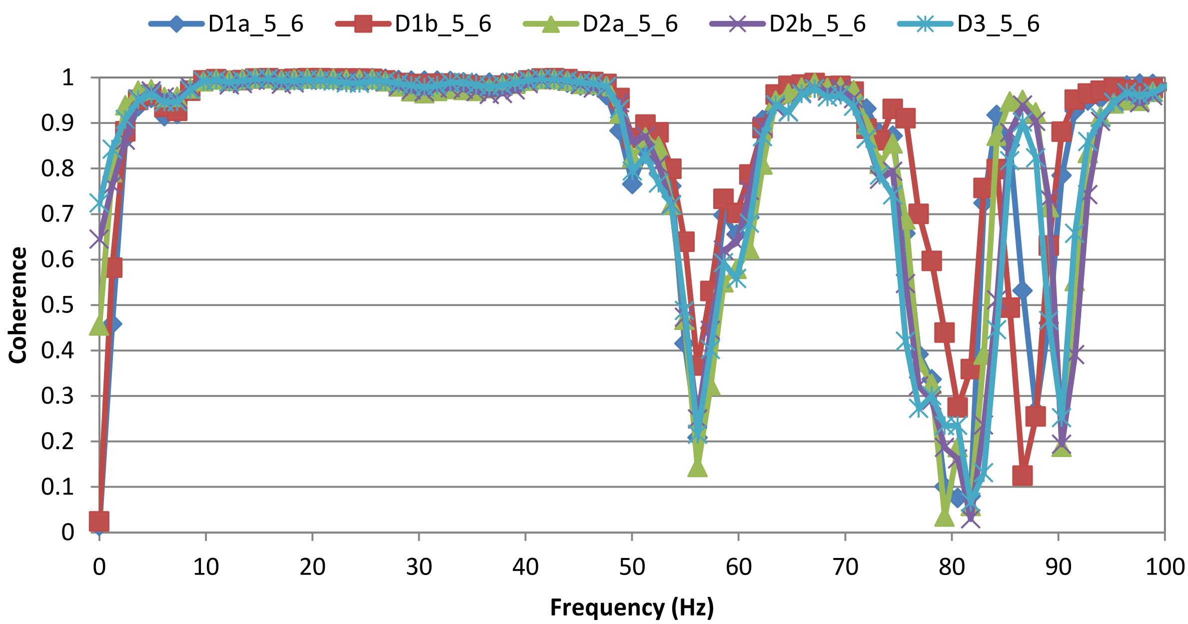

Figure 18. Coherence for pair of Sensors 5 and 6

The coherence for the other pairs of sensors investigated showed very similar values; therefore, these plots are included in the appendix rather than here. Figure 19 shows the results of these transient analyses as compared to the 50 impacts taken before Damage 1.

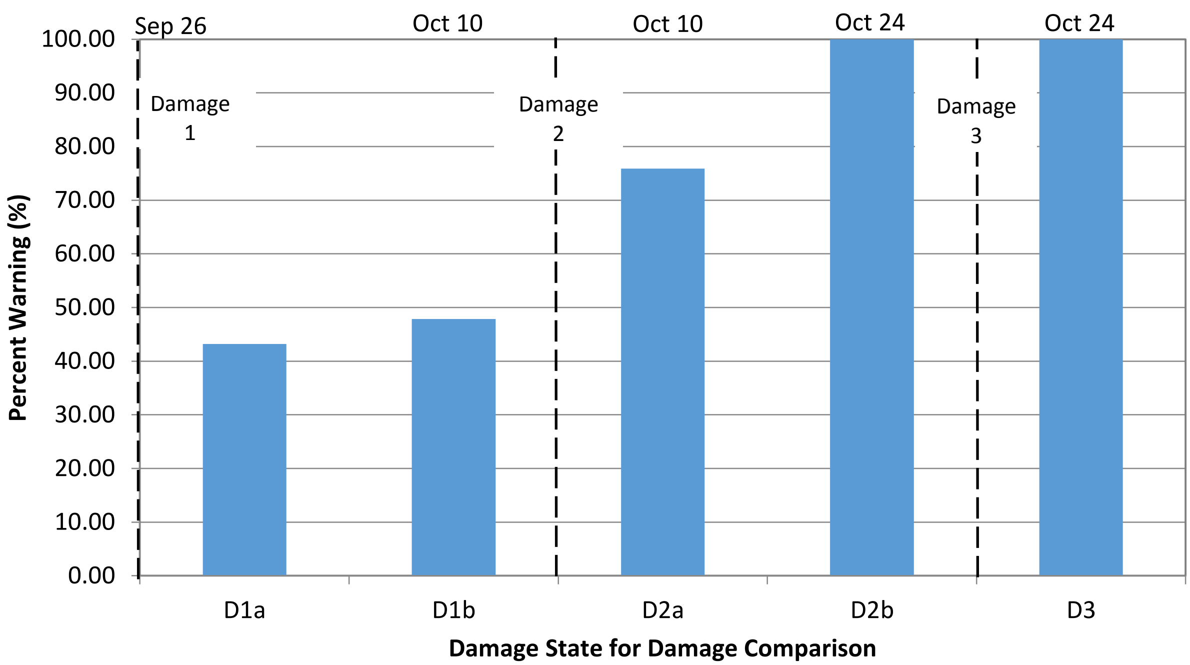

See Figure 17 for sensor locations

Figure 19. Percent warnings of manual impacts for multiple damage states compared to baseline damage state for the sacrificial specimen

The notation used in this figure is as follows: the number (1, 2, or 3) represents the damage state, the lowercase letter “a” represents the 50 impacts directly after the damage for that damage state, and the lowercase letter “b” represents the 50 impacts directly before the next damage state (two weeks after D#a).

The expectation from these results was that each separate damage state should give a similar percent warning (i.e., D1a should be similar to D1b) and that the percent warning should increase with damage (i.e., D1b should be smaller than D2a). As expected, damage is clearly detected (all damage states are above the 10 percent buffer limit), and damage is nearly quantified in that D2 is larger than D1. Because the percent warning cannot exceed 100 percent, any difference or quantification between D2 and D3 is not visible when comparing results to the baseline data.

After showing that the algorithm works on the sacrificial specimen for manual impacts, the algorithm was then used to determine whether or not damage could be detected by using traffic data. This traffic data was gathered in parallel with the transient analyses, providing two weeks of data for each damage state. Due to some unforeseen error in transmission, days in which the majority of the one-minute files were missing were not included in the analysis, which explains why there are not 14 days for each damage state shown in the results. Figure 20 shows the percent warnings for each day compared to the baseline. As shown, the healthy days are within the acceptable buffer of 10 percent, and all other days clearly detect damage (>10 percent) in the sacrificial specimen.

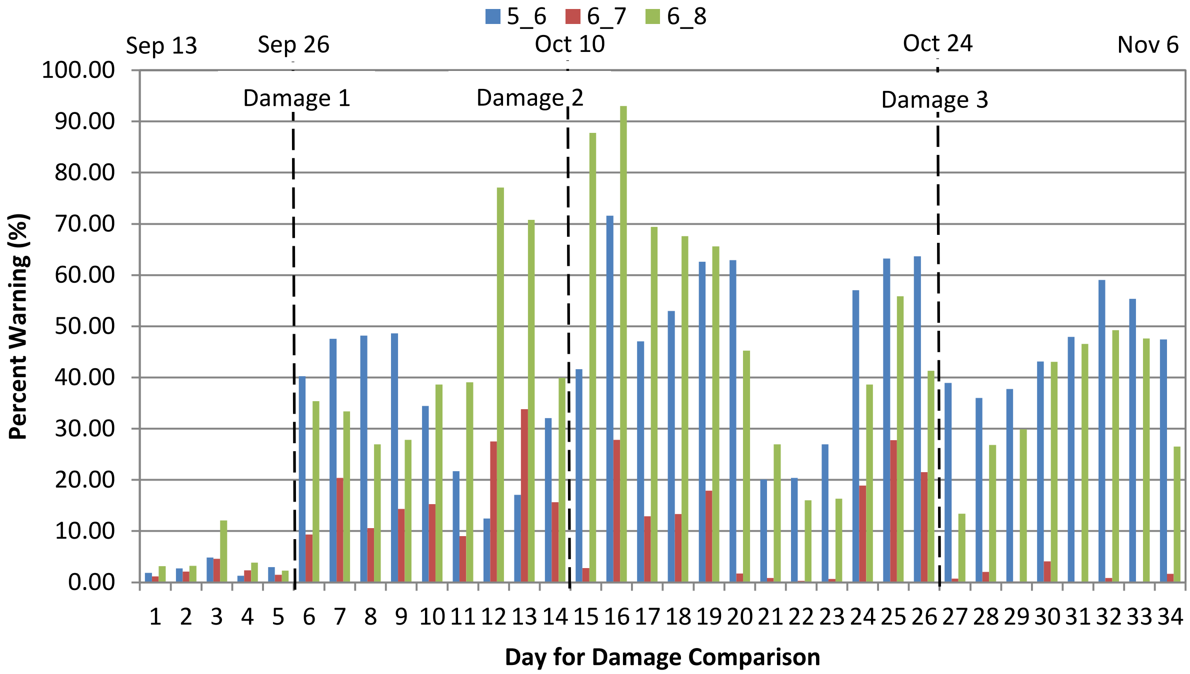

See Figure 17 for sensor locations

Figure 20. Percent warnings of traffic data for multiple days compared to baseline day for the sacrificial specimen

Damage quantification was unsuccessful for this analysis due to the inconsistencies in the percent warnings. However, initial investigation showed an association between percent warning and temperature changes. The temperature is averaged over the same 24 hour period for the comparison to the baseline data, and each comparison day's average temperature is shown in Figure 21.

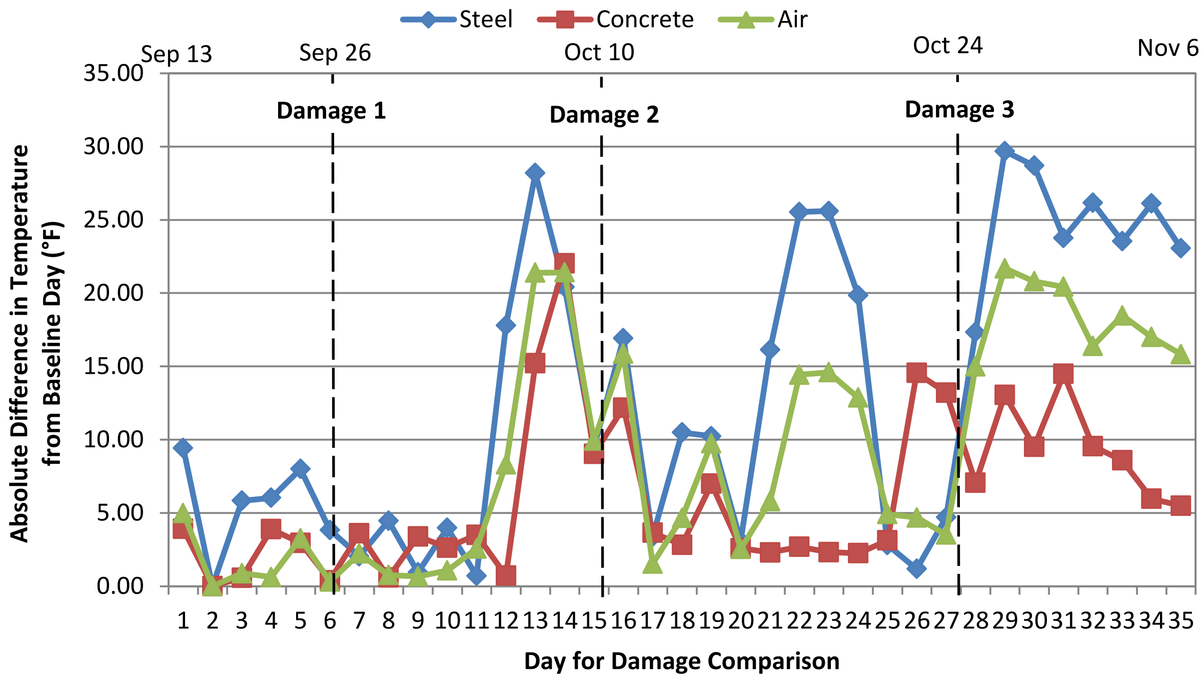

Figure 21. Absolute differences in average daily temperatures from the baseline day for the sacrificial specimen

The association between percent warning and temperature changes suggests that for any significant change in temperature between days (or during the same day), a similarly significant change occurs within the warning percentage. Further investigation is required to better understand the relationship between temperature and damage quantification.

5. CONCLUSIONS AND RECOMMENDATIONS

The transmissibility concept and damage-detection algorithm presented in this report demonstrate the potential to sense local changes in the dynamic stiffness between points across a joint of a real structure. Because the majority of failures occur at or near a connection, knowing the changes in inertial properties of failure-critical joints on a bridge would greatly improve detection capabilities and could prevent catastrophic failure.

The vibration-based algorithm was tested and validated as follows:

- Laboratory experiments on a connection specimen using transient loading conditions
  - Warning percentages detected, quantified, and located damage
  - Percent warnings had difficulties in quantifying magnitudes of damage (could not exceed 100 percent)

- Field testing on a sacrificial specimen that was geometrically similar to the laboratory connection specimen
  - Warning percentages detected damage under normal traffic loading
  - Environmental effects (temperature, wind, construction, etc.) were believed to cause false damage results
  - Quantification of damage was unsuccessful due to variations caused by environmental effects

- Field testing of joints near the mid-span and quarter-span of a bridge girder
  - Warning percentages were utilized on bridge connections directly with substantial significance
  - False damage was detected when significant changes in temperature occurred and during construction of a trail under the bridge

This study showed that the presented algorithm is successful in experimental testing and that it has great potential for application in field analysis.

The association between percent warning and temperature changes suggests that for any significant change in temperature between days (or during the same day), a similarly significant change occurs within the warning percentage. Further investigation is required to better understand the relationship between temperature and damage quantification. Overall, the presented algorithm was successful at detecting damage for days in which temperatures remained near stationary; therefore, this algorithm could benefit from supplementary temperature information to negate false warnings.

With further investigation to expand the understanding of how temperature affects warning percentages, future work could entail temperature compensation within the damage-detection algorithm or provision of supplemental temperature information to add redundancy to the procedure.

It should also be noted that during the investigation of the field specimen and bridge, construction of a trail occurred directly underneath the bridge. Although the exact start date of construction is unknown, it is reasonably estimated that construction equipment was being used from around October 23 through the middle of November. This construction equipment added noise and ambient vibrations to the entire system (bridge, sacrificial specimen, and surrounding area) that could account for the false damage readings seen in Figures 19, 20, and 12. Although it is not definite that this construction is the cause for the false damage detections, the vibrations were significant enough to warrant discussion.

The validation and integration of the vibration-based and strain-based damage-detection methodologies will add significant value to Iowa's current and future bridge maintenance, planning, and management.

REFERENCES

Adewuyi, A. P., Wu, Z., and Serker, N. H. M. K. (2009). "Assessment of Vibration-Based Damage Identification Methods Using Displacement and Distributed Strain Measurements." *Structural Health Monitoring*, August 2009. 8(6), 443-461.

Baker, M., and Lowy, J. (2013). "Thousands of Bridges at Risk of Freak Collapse." *Associated Press*, Seattle.

Chang, P. C., Flatau, A., and Liu, S. C. (2003). "Health Monitoring of Civil Infrastructure." *Journal of Structural Health Monitoring*, 2(3), 257-267.

Chesne, S., and Deraemaeker, A. (2013). "Damage Localization Using Transmissibility Functions: A Critical Review." *Mechanical Systems and Signal Processing*, 28, 569-584.

Devriendt, C., and Guillaume, P. (2008). "Identification of Modal Parameters from Transmissibility Measurements." *Journal of Sound and Vibration*, 314, 343-356.

Doebling, S. W., Farrar, C. R., Prime, M. B., and Shevitz, D. W. (1996). *Damage Identification and Health Monitoring of Structural and Mechanical Systems from Changes in their Vibration Characteristics: A Literature Review*. Los Alamos National Laboratory Report.

Ewins, D. J. (2000). *Modal Testing: Theory, Practice and Application, Second Edition*, Philadelphia: Research Studies Press Ltd. Print.

Guo, G. Q., Xiaozhai, Q., Dong, W., and Chang, P. (2005). "Local Measurement for Structural Health Monitoring." *Earthquake Engineering and Engineering Vibration*, 4(1), 165-172.

Johnson, T. J. and Adams, D. E. (2002) "Dynamic Transmissibility as a Differential Indicator of Structural Damage" *Journal of Vibration and Acoustics*., American Society of Mechanical Engineering. Vol. 124, No. 4, 634-641.

Maia, N. M. M., Almeida, R. A. B., Urgueira, A. P. V., and Sampaio, R. P. C. (2011a). "Damage Detection and Quantification Using Transmissibility." *Mechanical Systems and Signal Processing*, 25, 2475-2483.

Maia, N. M. M., Urgueira, A. P. V., and Almeida, R. A. B. (2011b). *Whys and Wherefores of Transmissibility*. Vibration Analysis and Control – New Trends and Developments, Dr. Francisco Beltran-Carbajal (Ed.), ISBN: 978-953-307-433-7, InTech.

Maia, N. M. M., Silva, J. M. M., and Ribeiro, A. M. R. (2001). "The Transmissibility Concept in Multi-Degree-of-Freedom Systems." *Mechanical and Signal Processing*, 15, 129-137.

Phares, B. M., Wipf, T. J., Lu, P., Greimann, L., and Pohlkamp, M. (2011). *An Experimental Validation of a Statistical-Based Damage-Detection Approach*. Bridge Engineering Center, Iowa State University, Ames, Iowa. January 2011.

Ribeiro, A. M. R., Silva, J. M. M., and Maia, N. M. M. (2000). "On the Generalization of the Transmissibility Concept." *Mechanical and Signal Processing*, 14, 29-35.

Rytter, A. (1993). *Vibration Based Inspection of Civil Engineering Structures*. PhD thesis, Department of Building and Structural Engineering, Aalborg University, Denmark.

Schulz, M. J., Abdelnaser, A. S., Pai, P. F., Linville, M. S., and Chung, J. (1997). *Detecting Structural Damage Using Transmittance Functions*. International Modal Analysis Conference, Orlando, Florida. 638-644.

U.S. DOT. (2012). *Deficient Bridges by State and Highway System 2012*. Last accessed October 4, 2013. Available at: www.fhwa.dot.gov/bridge/nbi/no10/defbr12.cfm.

Weijtjens, W., De Sitter, G., Devriendt, C., and Guillaume, P. (2013). "Relative Scaling of Mode Shapes Using Transmissibility Functions." *Mechanical Systems and Signal Processing*, 40, 269-277.

APPENDIX A. COHERENCE FOR ADDITIONAL PAIRS OF SENSORS FOR SACRIFICIAL SPECIMEN

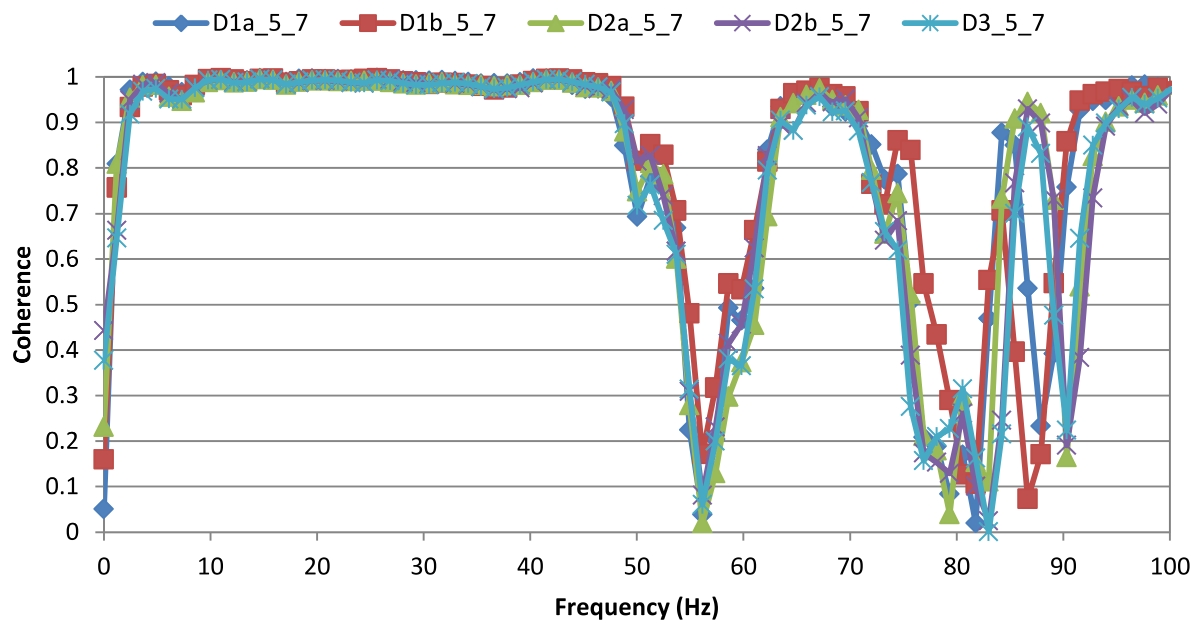

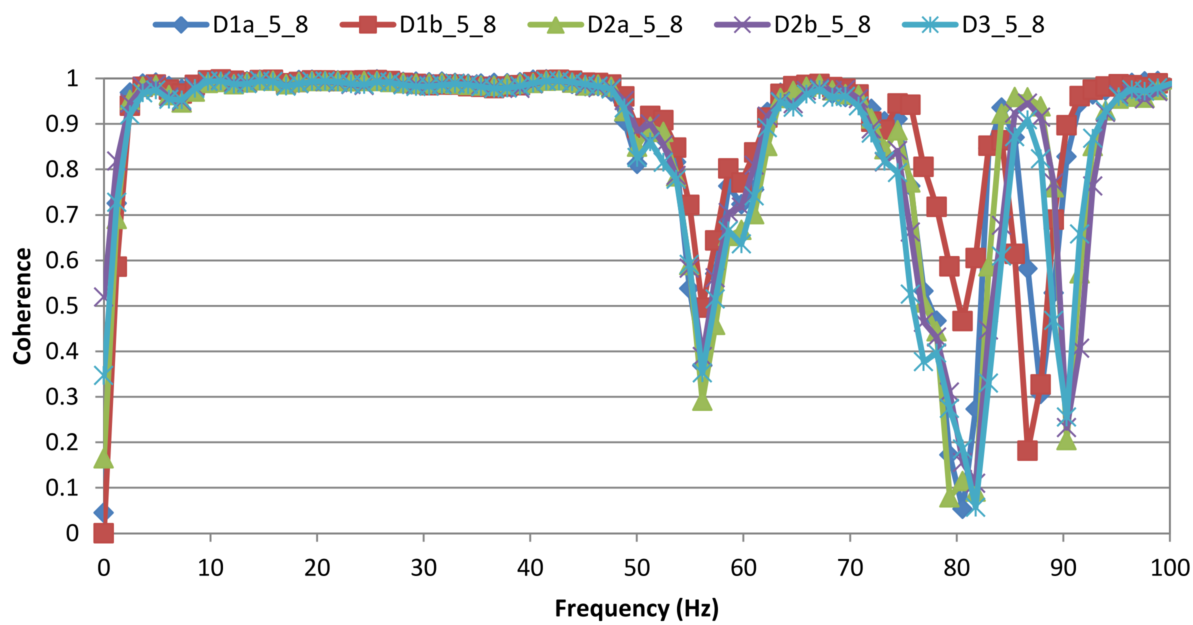

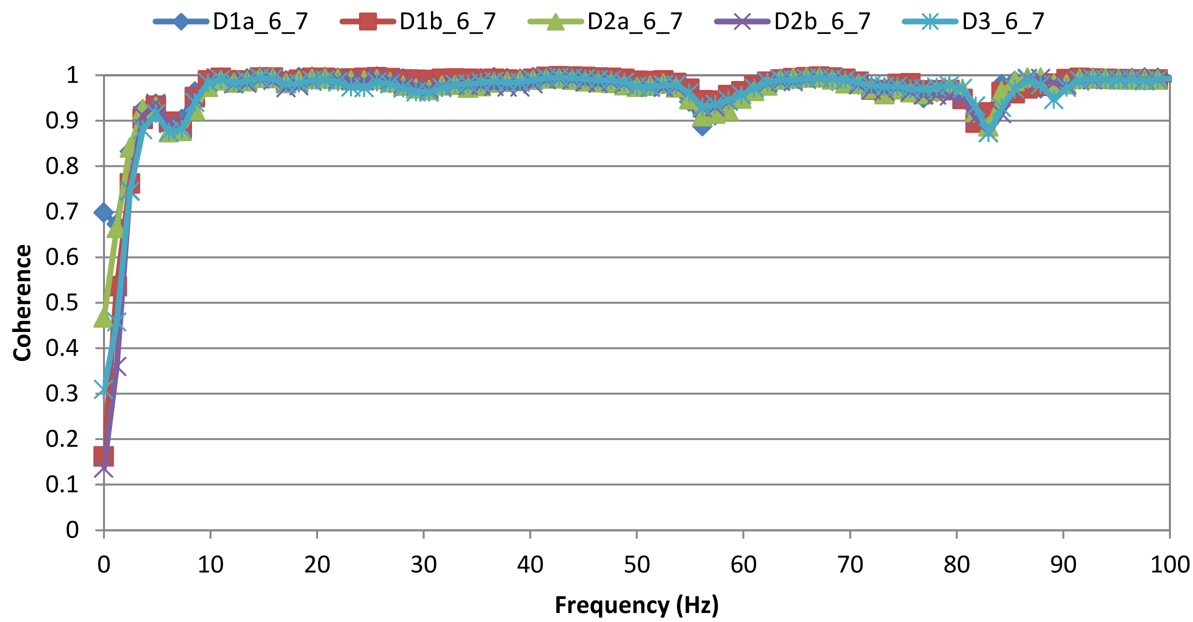
D1a_6_7
D1b_6_7
D2a_6_7
D2b_6_7
D3_6_7
Coherence
Frequency (Hz)

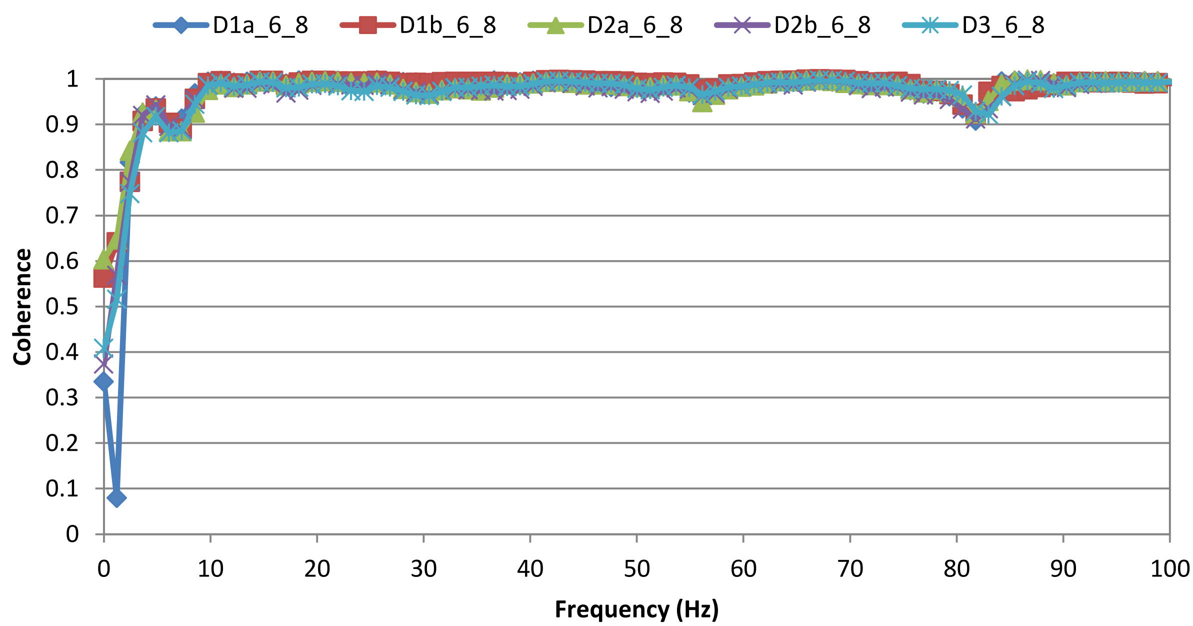
D1a_6_8
D1b_6_8
D2a_6_8
D2b_6_8
D3_6_8
Coherence
Frequency (Hz)